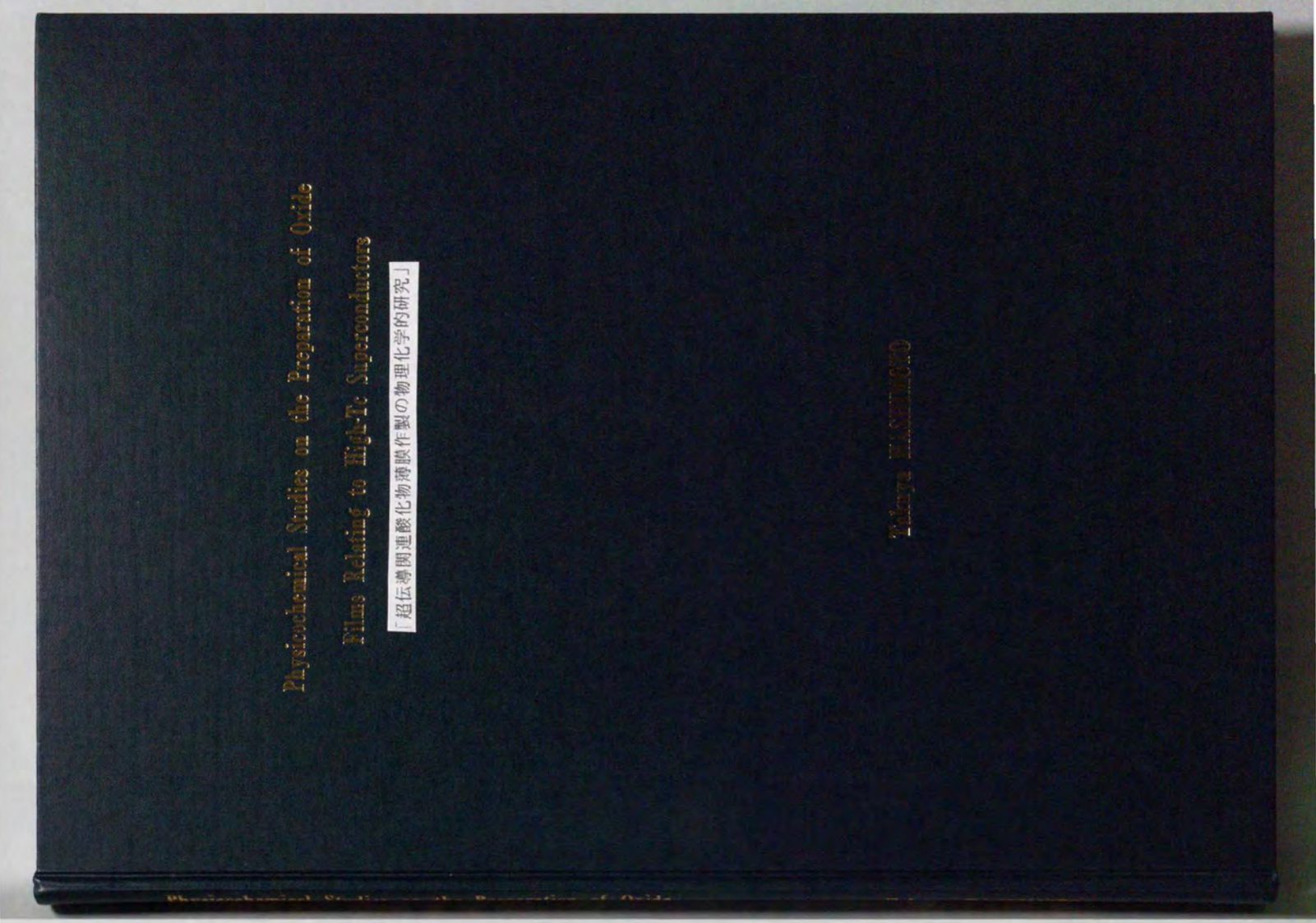
Physicochemical Studies on the Preparation of Oxide
Films Relating to High-Tc Superconductors
「超伝導関連酸化物薄膜作製の物理化学的研究」
Takao KANAMOTO

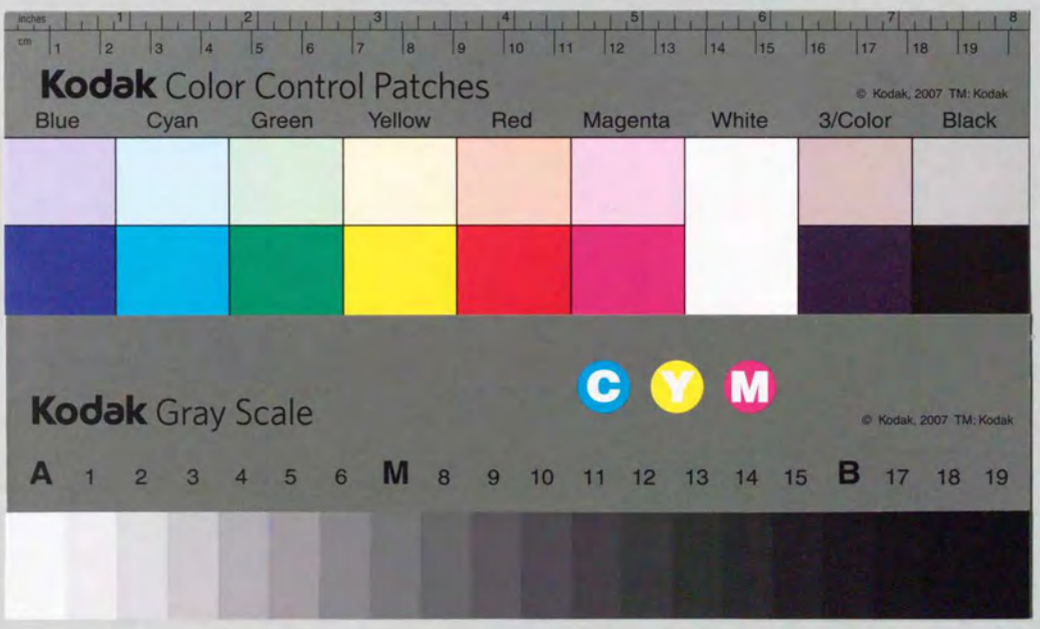
Kodak Color Control Patches
© Kodak, 2007 TM: Kodak
Blue
Cyan
Green
Yellow
Red
Magenta
White
3/Color
Black
Kodak Gray Scale
© Kodak, 2007 TM: Kodak
A
B
M

(1)

PHYSICOCHEMICAL STUDIES ON THE PREPARATION OF OXIDE FILMS RELATING TO HIGH-Tc SUPERCONDUCTORS

TAKUYA HASHIMOTO

Graduate Course of Chemical Energy Engineering

University of Tokyo

January, 1991

PREFACE

The present thesis is the collection of the studies which have been carried out under the direction of Prof. Hideomi Koinuma during 1987-1990. The studies are concerned with preparation of oxide relating to high-T_c superconducting films. In this study, screen-printing/sintering was examined as a method for the preparation of superconducting thick films. The physical and chemical interactions between superconduicting film and substrate was estimated semi-quantitatively. In addition, low temperature synthesis of oxide films was investigated by plasma and photo chemical vapor deposition.

The author would like to express his deepest gratitude to Prof. Hideomi Koinuma for his valuable advice and continuous encouragement throughout the work.

The author also would like to express his gratitude to Prof. Koichi Kitazawa and Prof. Kazuo Fueki who encourage him to work in the field.

The author is grateful to Dr. M. Kawasaki, Dr. K. Kishio, Dr. T. Hasegawa, Dr. Y. Yoshida, Dr. M. Takata, Prof. Y. Okabe, Prof. T. Shiraishi, Dr. M. Kogoma, Dr. S. Okazaki, Prof. T. Yamamoto, Dr. K. Sato, Dr. Y. Takagi, Prof. A. B. Sawaoka, Prof. M. Kawai, Miss R. Sekine, Mr. T. Sung, Dr. S. Okazaki, Prof. O. Odawara, Prof. T. Hirano, Mr. M. Funabashi, Mr. T. Manako and Dr. M. Yoshimoto for their fruitful discussions.

The author is much indebted to Mr. N. Takahashi, Mr. T. Nakamura, Mr. T. Kosaka, Dr. S. Nagata, Miss K. Masubuchi, Dr. M. Kudo, Mr. A. Kishi, Mr. T. Azumi, Mr. A. Inoue, Mr. T. Yoshida, Mr. T. Asakawa, Mr. K. Fukuda, Mr. Y. Suemune, Mr.

M. Nakabayashi, Mr. K. A. Chaudhary, Mr. Y. Takemura, Mr. T. Nagai, Mr. K. Inomata, Mr. H. Sakurai, and Mr. H. Nagata for their active collaboration in the course of the study.

Messrs. A. Takano, S. Gonda, T. Tsukahara, M. Nakano, K. Takeuchi, Y. Saito, T. Nakajima, Y. Matsuzaki, Y. Sato. M. Sasaki, M. Fujishima, K. Hashida, S. Uchida, M. Sumiya, H. Ohkubo, M. Matsuse, S. Nakanishi and many other members of Koinuma Laboratory and Fueki-Kitazawa Laboratory offered the author many helpful suggestions and kind assistance, for which the author is deeply grateful.

Finally the author expresses his deep gratitude to members of Aikido Club of University of Tokyo for their support to daily life and his parents for their support in all means.

January, 1991

Takuya Hashimoto

CONTENTS

Chapter 1

General Introduction

Film preparation of high-T_c superconducting oxide have been attracting much interest from the viewpoint of not only practical application such as devices using Josephson junction, thermal sensor and shielding of magnetic field but also elucidation of physical and electrical properties deriving from anisotropic structure of the superconductor.[1] Superconducting films have been successfully prepared by dc-sputtering[2], rf-magnetron sputtering[3], molecular beam epitaxy[4], laser ablation[5], chemical vapor deposition[6], spin coating[7], screen printing[8] and so on. However, few report have appeared on the interactions between superconducting films and substrate which must be considered in order to prepare high-T_c or high-J_c film.

In addition, it is expected that high-T_c and high-J_c film is synthesized by using artificial layer-by-layer deposition since superconducting oxides have two-dimensional atomically layered structure as Fig. 1-1 shows.[9] For example, Bi-Sr-Ca-Cu-O superconducting system has a structure of several number of Ca/CuO_2 bi-layers sandwiched by two Bi_2O_2/SrO stacked layers. Furthermore, construction of new layered structures with some new physical or electrical properties which is thermodynamically unstable may be possible by an application of layer-by-layer deposition. So far, construction of multilayered film by physical vapor deposition such as molecular beam epitaxy,[10] laser ablation,[11] and sputtering[12] have been reported. Although chemical vapor deposition (CVD) is the most promising for layer-by-layer deposition due to its high controllability and

possibility of low temperature process, its application to artificial construction of atomically layered structure has not been reported.

The author successfully prepared high-T_c superconducting thick films by screen printing method at the first time of the world. Also evaluated were the physical and chemical interactions between superconducting oxide and substrate materials, such as mismatch of thermal expansion coefficients and solid phase reactions, which must be considered in order to prepare high quality film. The author also studied low temperature synthesis of oxide films relating to high-T_c superconductor by plasma CVD as a fundamental method for artificial construction of atomically layered ceramic structure. The studies are extended to the purification method and UV-VIS absorption properties of CVD sources and to low temperature oxide film synthesis by photo CVD.

The dissertation consists of seven chapters. Chapter 2 presents preparation of superconducting thick films by screen printing method. Superconducting thick film was successfully prepared at first time using optimum substrate and sintering conditions. In chapter 3, interaction between superconducting oxide and substrate materials are examined semi-quantitatively. Chapter 4 presents low temperature preparation of oxide film by chemical vapor deposition using microwave plasma and rf plasma. In chapter 5, purification and UV-VIS light absorption of source materials for CVD of high-T_c superconductors are investigated. The data are indispensable to photo CVD of oxide films. Chapter 6 presents low temperature synthesis of Bi, Sr, Ca, Cu and Ca-Cu

oxide films by photo CVD using low pressure mercury lamp. In chapter 7, general summary of this study is presented.

References

1) For example, H. Koinuma: Pure and Appl. Chem. 60 (1988) 715.

2) H. Koinuma, M. Kawasaki, M. Funabashi, T. Hasegawa, K. Kishio, K. Kitazawa and K. Fueki: J. Appl. Phys., 62 (1987) 1524.

3) Y. Enomoto, T. Murakami, M. Suzuki and K. Moriwaki: Jpn. J. Appl. Phys., 26 (1987) L1248.

4) J. Kwo, T. C. Hsieh, R. M. Fleming, M. Hong, S. H. Liou, B. A. Davidson and L. C. Feldman: Phys. Rev. B64 (1987) 4039.

5) D. Dijkkamp, T. Venkatesan, X. D. Wu, S. A. Shaheen, N. Jisrawi, Y. H. Min-Lee, W. L. MacLean and M. Croft: Appl. Phys. Lett., 51 (1987) 8822.

6) H. Yamane, H. Kurosawa and T. Hirai: Chem. Lett., 1988 (1988) 939.

7) S. L. Furcone and Y. M. Chiang: Appl. Phys. Lett., 52 (1988) 2180.

8) H. Koinuma, T. Hashimoto, M. Kawasaki and K. Fueki: Jpn. J. Appl. Phys., 26 (1987) L399.

9) L. H. Greene: The 5th Seminar on Frontier Technology-Chemcal Aspects of High-T_c Superconductors- The Association for the Progress of New Chemistry June 7-10 (1988) in Shuzenji: Y. Tokura and T. Arima, Jpn. J. Appl. Phys., 29 (1990) 2388.

10) E. S. Hellman, D. G. Schlom, A. F. Marshall, S. K. Streiffer, J. S. Harris, Jr., M. R. Beasely, J. C. Bravman, T. H. Geballe, J. N. Eckstein and C. Webb: J. Mater. Res., 4 (1989) 476.

11) H. Tabata, T. Kawai, M. Kawai, O. Murata and S. Kawai: Jpn. J. Appl. Phys., 28 (1989) L823.

12) H. Adachi, S. Kohiki, K. Setsune, T. Mitsuyu and K. Wasa: Jpn. J. Appl. Phys., 27 (1988) L1883.

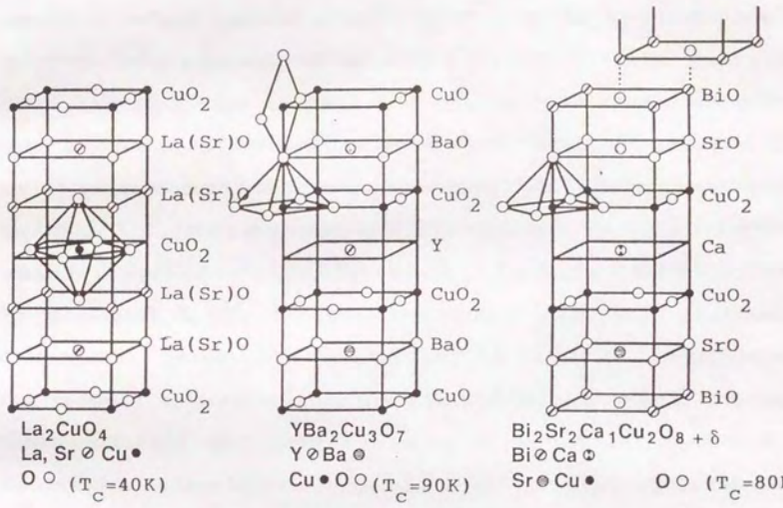

Fig. 1-1. Crystal structures of representative high-T_c superconductors.

Chapter 2

Screen-Printing/Sintering as a Preparation Method of Oxide Superconducting Films

2-1. Introduction

Film preparation of high-T_c superconducting oxides has been attracting much interest from the viewpoints not only of electronic device application but also of the elucidation of basic properties of superconducting oxides. A lot of papers have already been reported on the preparation of superconducting films by such methods as sputtering,[1] vacuum evaporation,[2] laser ablation,[3] and molecular bean epitaxy.[4] However, these processes require high vacuum reactors and it is difficult to prepare films of large areas. Compared to these processes, screen-printing/sintering method is a simple low cost process and has been verified to be suitable for preparing CdS/CdTe solar cells, metallic patterns for interconnecting electronic circuits and so on.[5] As soon as the high-T_c superconductivity of La-M-Cu-O (M= Ca, Sr, Ba) system had been confirmed, [6,7] the author started his research on making films of new high-T_c superconductors by screen-printing/sintering method.[8-11] This chapter describes studies on the preparation of thick films by screen-printing/sintering method, and presents preliminary data on physical and chemical interactions between the superconductors and substrate materials.

2-2. Experimental

Figure 2-1 depicts the flow chart of preparation of superconducting film by screen-printing method. The powders of superconducting oxides, $(La_{0.9}Sr_{0.1})_2CuO_{4-\delta}$(LSCO), $Ba_2YbCu_3O_{7-\delta}$(BYbCO) and Bi-Sr-Ca-Cu-O (BSCCO) were prepared by grinding in an agate mortar the sintered mixed powders of component metal oxides and carbonates. The paste, i.e. the ink for printing was prepared by mixing the superconducting powder and such an organic vehicle as hepthyl alcohol, octhyl alcohol and propylene glycol and it was printed on several kinds of substrates (quartz, alumina, YSZ, $SrTiO_3$ and La_2CuO_4) through a 150mesh silk screen. The printed film was dried in vacuo at 150°C for more than 6h and then fired in a furnace for being sintered. The heat treatment conditions employed for various superconducting films were summarized in Table 2-1. The sintered film thicknesses were determined to be 10±2μm from the observation of film cross section by an optical microscope. The crystal structure of the films was determined by the X-ray diffraction analysis using a Rigaku RAD2C diffractometer. Surface state of the films was observed by an optical microscope. Resistivity vs. temperature relationship was measured by the conventional dc four probe method on rectangular specimens of the films. Four gold terminals were evaporated on a film printed and sintered on a substrate whose size was about 14x7x1mm. Magnetic susceptibilitiy of some films was measured using a SQUID magnetometer SHE model 905.

2-3. Results and Discussion

2-3-1. Superconductivity of screen printed films.

Table 2-1 shows representative results of film preparation, together with the preparation conditions. As Fig. 2-2 and Fig. 2-3 show, zero resistivity of screen-printed and sintered film were achieved at 7K for LSCO printed on YSZ and at 22K for LSCO on

La_2CuO_4, and at 83K and 79K for BYbCO films on YSZ and on $SrTiO_3$, respectively. In case of BSCCO, zero resistivity was achieved at 11k and 68K on $SrTiO_3$ and YSZ, respectively as Fig. 2-4 and Fig. 2-5 show. The critical currents(J_c) of these superconducting films were relatively small as Fig. 2-6 shows. BYbCO film printed on YSZ showed superconducting at 77.2K at a current density of $0.02A/cm^2$. When the current density was increased to $14.2A/cm^2$, $T_{c,zero}$ decreased to 15.8K. The zero resistivity temperature ($T_{c,zero}$) and critical curent density (J_c) should be further increased by optimizing the sintering conditions. LSCO, BYbCO and BSCCO films printed on quartz became insulator by the heat-treatments for 1h and longer at temperatures of 1000 °C, 900 °C and 830 °C, respectively. Alumina appears to be a little better substrate than quartz, but it still was not satisfactory. LSCO films on alumina substrate showed resistivity drop at about 40K, but the resistivity did not reach zero even at 4.2K. BYbCO printed films were sintered at 900 °C for more than 2h to be insulators. A BSCCO film showed a semiconductive temperature dependence of resistivity when it was sintered at 830 °C for 1h.

2-3-2. Interaction between substrate and superconductors

The observed strong dependence of superconductivity of printed and sintered films on substrate material prompted the author to evaluate the interaction between the superconductors and substrate materials in order to interpret the above results and to search for other appropriate substrates.

One of the interactions which must be taken into account is solid state chemical reactions between the substrate materials

and the superconductors at high temperatures. When LSCO and BSCCO films on quartz substrates were sintered at 1000° C for 1h and at 830 °C for 1h, respectively, the films changed their color from black to greenish black and turned to be insulators. Figure 2-7 and Figure 2-8 show that the X-ray diffraction patterns of these LSCO and BSCCO films, respectively. Heating LSCO film in air at 1000 °C for 10min made film-quartz interface grayish green although XRD pattern stayed substantially the same as the pattern of bulk $(La_{0.9}Sr_{0.1})_2CuO_{4-\delta}$. The whole film of about 10μm thick turned to be grayish green film by the heating for 1h and remarkable change in XRD pattern was accompanied as shown in Fig. 2-7(b). In the XRD pattern of sintered BSCCO film, the peaks assignable to CuO, $SrSiO_3$ and $CaSiO_3$ were newly observed in the X-ray pattern of the sintered film. Phase separation was also observed to occur around the interface between the film and such substrate as quartz, alumina and $SrTiO_3$ by the sintering of the screen printed superconducting oxide film. Figures 2-9 and 2-10 show XRD patterns of BYbCO and BSCCO films prepared on various substrates. In the XRD patterns of BYbCO film on quartz and alumina, peaks assigned to $BaCuO_2$ were predominant and both films turned to be insulating, while film on YSZ had a crystal structure assignable to superconducting BYbCO phase. In BSCCO film on alumina, the predominant crystal structure was $Bi_2Sr_2CuO_x$ (2201) phase, that is, so-called 20K or semiconducting phase. When $SrTiO_3$ and YSZ were used as substrates and films were sintered below 840°C, XRD patterns were almost same as that of bulk specimen. When sintering temperature was 850° C, crystal

structure of the film on $SrTiO_3$ was predominantly $Bi_2Sr_2CuO_x$ phase, while the film on YSZ had a predominant structure of $Bi_2Sr_2CaCu_2O_x$ phase which was superconductor with critical temperature of 80K.

Thermal expansion coefficient was another significant factor relating to the interaction between the superconductors and substrates. Although LSCO films prepared on alumina substrate maintained K_2NiF_4 structure in XRD, which was assigned to superconducting phase,[12] and showed Meissner effect (see Fig. 2-11), they did not give zero resistivity.(Fig. 2-12) This was due to crack formation on the film, which was observed by an optical microscope as Fig. 2-13 shows. This crack formation should be originated from a mismatch in thermal expansion coefficients of the superconducting oxides(LSCO: $1.4\times10^{-5}\,°C^{-1}$) and alumina($0.7\times10^{-5}\,°C^{-1}$).[13]

2-4. Conclusion

LSCO, BYbCO and BSCCO superconducting thick films were prepared by a simple screen-printing/sintering method. Chemical and physical interactions between various superconductors and substrates must be taken into account for the preparation of superconducting film. YSZ and $SrTiO_3$ are preferable substrate materials to quartz and alumina.

References

1) M. Kawasaki, S. Nagata, Y. Sato, M. Funabashi, T. Hasegawa, K. Kishio, K. Kitazawa, K. Fueki and H. Koinuma: Jpn. J. Appl. Phys., 26 (1987) L738.

2) R. B. Laibowitz, R. H. Koch, P. Chaudhary and R. J. Gambino: Phys. Rev., B35 (1987) 8822

3) M. Kanai, T. Kawai, M. Kawai and S. Kawai: Jpn. J. Appl. Phys., 26 (1988) L1746.

4) D. G. Schlom, J. N. Eckstein, E. S. Hellman, S. K. Streiffer, J. S. Harris, Jr., M. Beasely, J. C. Bravman, T. H. Geballe, C. Webb, K. E. Dessonneck and F. Turner: Appl. Phys. Lett., 53 (1989) 1660.

5) H. Matsumoto, N. Nakayama and S. Ikegami: Jpn. J. Appl. Phys., 19 (1980) 129.

6) S. Uchida, H. Takagi, S. Tanaka and K. Kitazawa: Jpn. J. Appl. Phys., 26 (1987) L1.

7) K. Kishio, K. Kitazawa, S. Kanbe, I. Yasuda, N. Sugii, H. Takagi, S. Uchida, K. Fueki and S. Tanaka: Chem. Lett., 1987 (1987) 429.

8) H. Koinuma, T. Hashimoto, M. Kawasaki and K. Fueki: Jpn. J. Appl. Phys., 26 (1987) L399.

9) H. Koinuma, T. Hashimoto, T. Nakamura, K. Kishio, K. Kitazawa and K. Fueki: Jpn. J. Appl. Phys., 26 (1987) L761.

10) T. Hashimoto, T. Kosaka, Y. Yoshida, K. Fueki and H. Koinuma: Jpn. J. Appl. Phys., 27 (1988) L384.

11) H. Koinuma and T. Hashimoto: Annual Res. Rep. of the Eng. Res. Inst., Fac. of Eng., Univ. of Tokyo, 47 (1988) 139.

12) H. Takagi, S. Uchida, K. Kitazawa and S. Tanaka: Jpn. J. Appl. Phys., 26 (1987) L123.

13) T. Hashimoto, K. Fueki, A. Kishi, T. Azumi and H. Koinuma: Jpn. J. Appl. Phys., 27 (1988) L214.

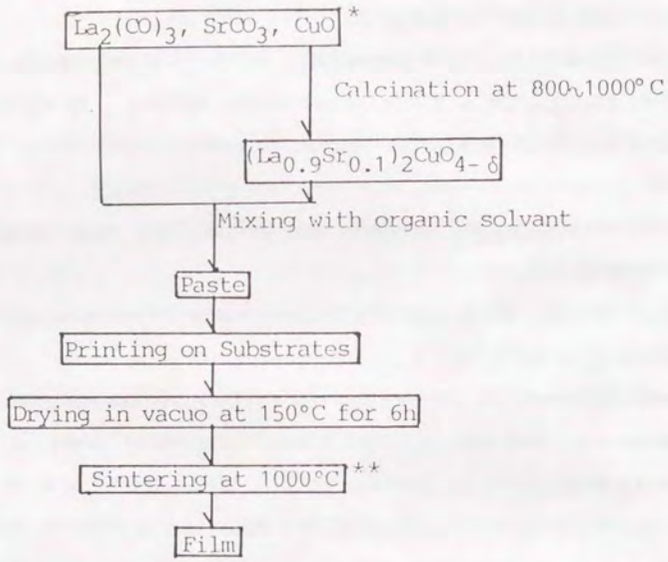

Fig. 2-1. Flow chart of superconducting film preparation by screen printing method.

* $BaCO_3$, Ln_2O_3, and CuO were used instead for $LnBa_2Cu_3O_{7-\delta}$. For Bi-Sr-Ca-Cu-O, Bi_2O_3, $SrCO_3$, $CaCO_3$, and CuO were used.

** Sintering temperature were 900 C for $LnBa_2Cu_3O_{7-\delta}$, 830°C∿850°C for Bi-Sr-Ca-Cu-O.

Table 2-1. Preparation conditions and properties of screen printed films.

	Superconductor	Substrate	Sintering Condition	Resistivity at r.t.	$T_{c,zero}$
#1	LSCO	quartz	1000°C, 1h	$>10^2$	-
#2	LSCO	alumina	1000°C, 15min	7.4×10^{-2}	-
#3	LSCO	YSZ	1000°C, 10min	4.6×10^{-2}	7K
#4	LSCO	La_2CuO_4	1000°C, 10min	8.5×10^{-4}	22K
#5	BYbCO	quartz	900°C, 2h	$>10^2$	-
#6	BYbCO	alumina	900°C, 2h	$>10^2$	-
#7	BYbCO	YSZ	900°C, 2h	3.6×10^{-2}	77K
#8	BYbCO	YSZ	900°C, 5h	9.7×10^{-3}	83K
#9	BYbCO	$SrTiO_3$	900°C, 5h	2.2×10^{-2}	79K
#10	BSCCO	quartz	830°C, 1h	$>10^2$	-
#11	BSCCO	alumina	830°C, 1h	2.4×10^{-2}	-
#12	BSCCO	$SrTiO_3$	840°C, 1h	9.2×10^{-2}	11K
#13	BSCCO	$SrTiO_3$	850°C, 1h	6.6×10^{-3}	-
#14	BSCCO	YSZ	840°C, 1h	1.5×10^{-2}	35K
#15	BSCCO	YSZ	850°C, 1h	9.1×10^{-3}	68K

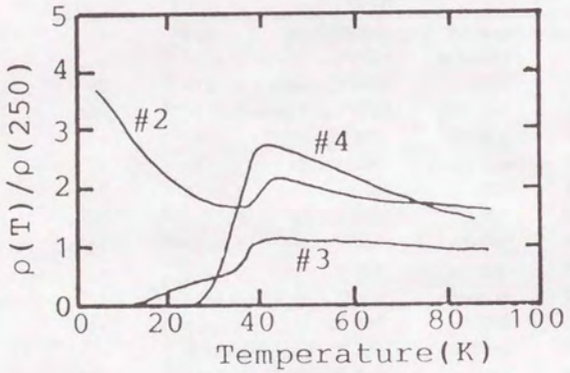

Fig. 2-2. Resistivity vs. temperature relationships for the screen printed and sintered LSCO films.

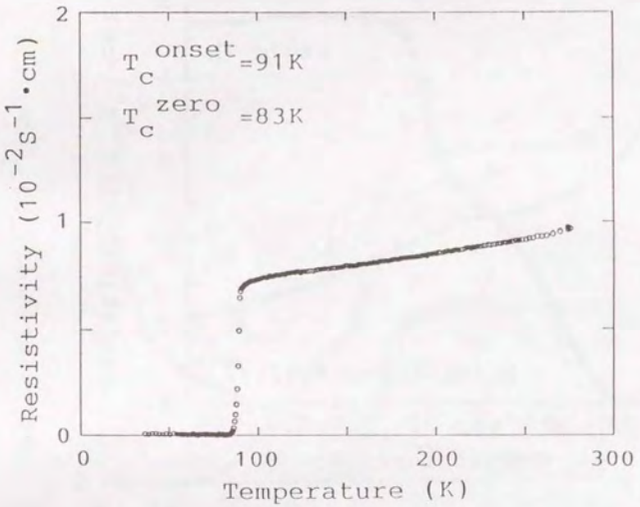

Fig. 2-3. Resistivity changes for the screen printed and sintered BYbCO film on YSZ as a function of temperature.

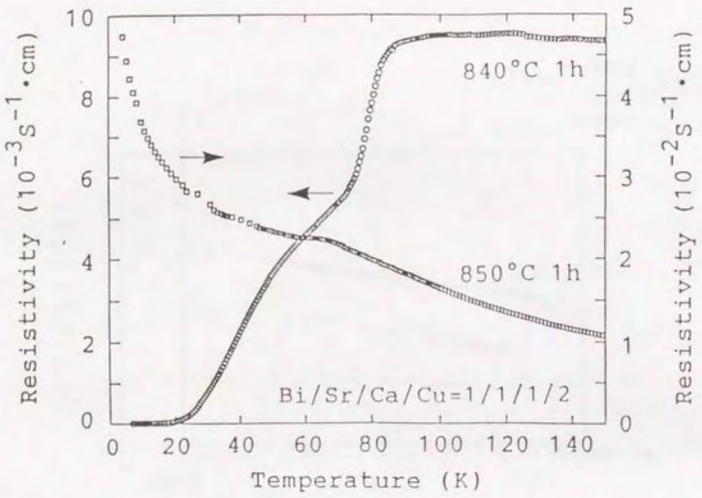

Fig. 2-4. Temperature dependences of resistivities for screen printed BSCCO film on $SrTiO_3$.

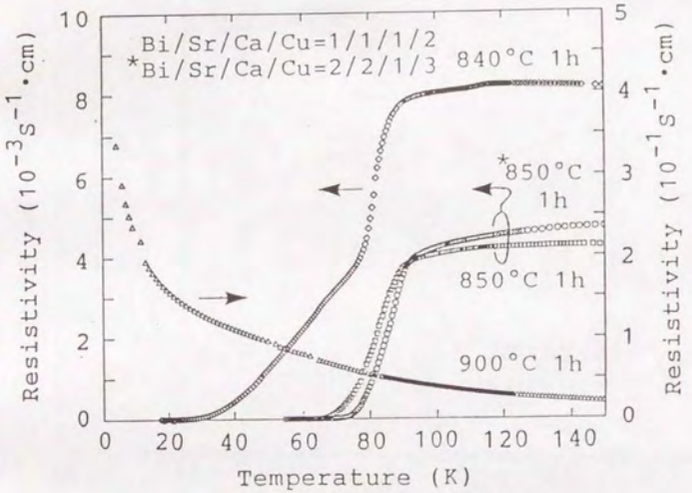

Fig. 2-5. Resistivity vs. temperature relationship for screen printed BSCCO films on YSZ.

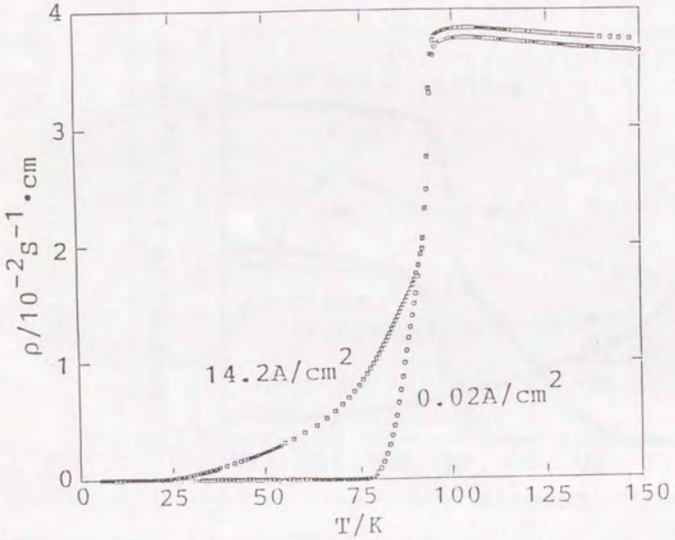

Fig. 2-6. Resistivity vs. temperature relationship for the BYbCO film on YSZ (specimen #7). Current density used for the measurement: ○ 0.02A/cm^2, □ 14.2A/cm^2.

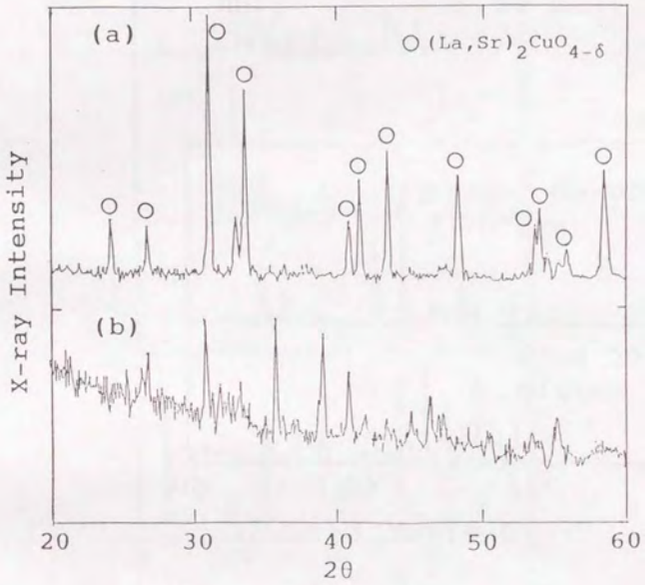

Fig. 2-7. X-ray diffraction patterns of LSCO films printed on quartz substrate and sintered at 1000 °C for 10min (a) and for 60min (b).

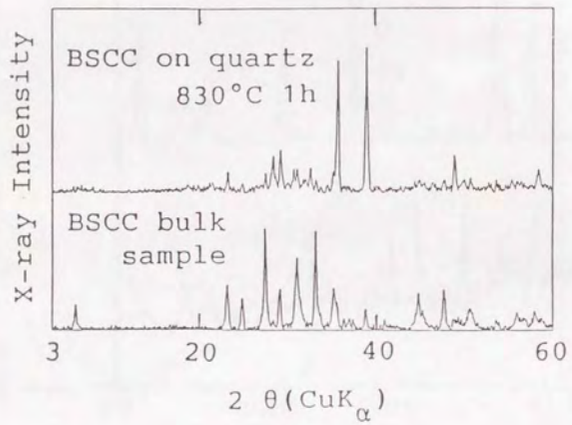

Fig. 2-8. XRD patterns of BSCCO screen printed film on quartz and bulk specimen.

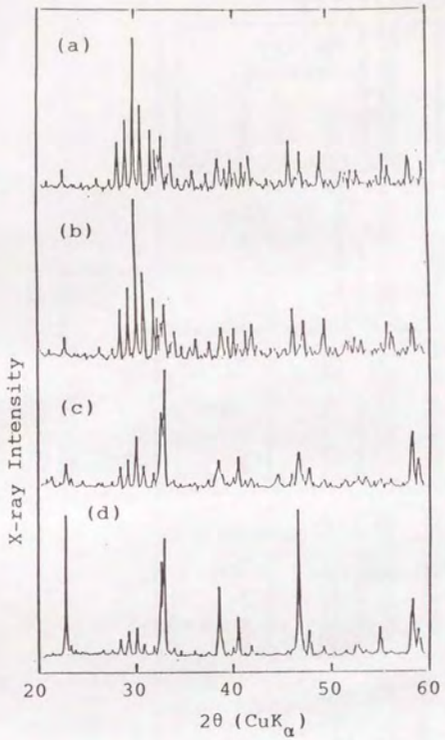

Fig. 2-9. XRD patterns of BYbCO films printed on quartz(a), alumina(b), and YSZ(c) substrate. The films were heat treated at 900 °C for 2h. The pattern of BYbCO superconducting bulk sample (d) is also shown for comparison.

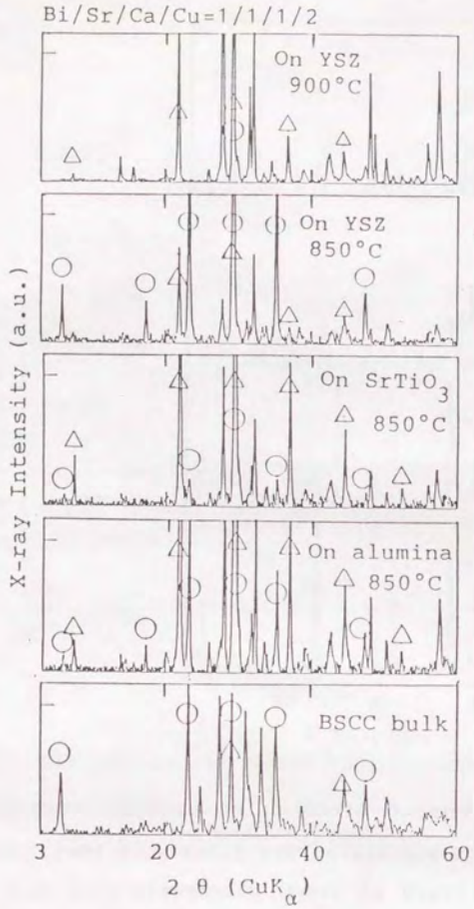

Fig. 2-10. XRD patterns of Bi-Sr-Ca-Cu-O films on several substrates and bulk specimen. Symbols represent the peaks corresponding to planar spacing of ○15.2/n A and △12.1/n A.

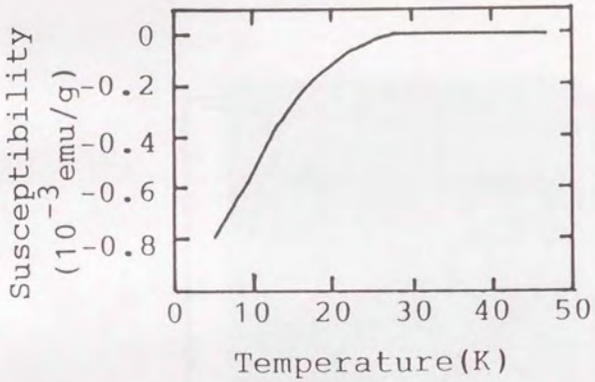

Fig. 2-11. Temperature dependence of the dc magnetic susceptibility of an LSCO film printed on alumina and heat-treated at 1000°C for 15min.

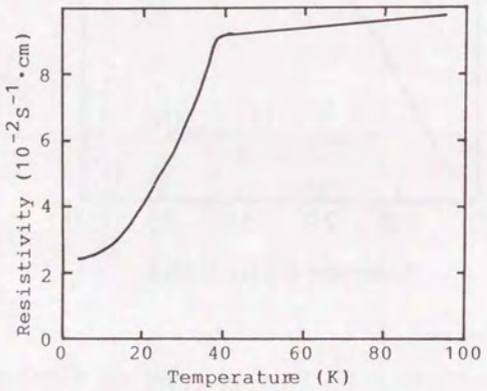

Fig. 2-12. Resistivity vs. temperature relationship for LSCO film printed on alumina.

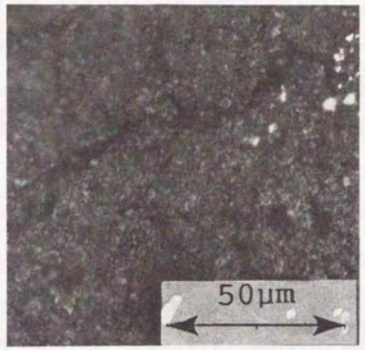

Fig. 2-13. Optical microscope image of LSCO film on alumina.

Chapter 3

Semi-quantitative Evaluation of Interaction between Superconductors and Substrate Materials

3-1. Introduction

In chapter 2, the author successfully prepared high-T_c superconducting films by screen-printing/sintering method and clarified qualitatively that chemical and physical interactions between superconducting oxides and substrate must be taken into consideration to obtain high-T_c superconducting film. Such interactions have been reported on the preparation of superconducting film by not only screen-printing/sintering but other technique. For example, Fig. 3-1 shows SEM images of LSCO film on glass (Corning #7059) prepared by sputtering and annealed at 590 ℃ for 15h. The cracks spreading the whole surface were observed. Resistivity drop was observed at about 40K, however, zero resistivity was not obtained in the film. (Fig. 3-2)[1] Chemical interactions, such as interdiffusions of elements, have also been investigated by Auger electron spectroscopy(AES),[2] secondary ion mass spectroscopy(SIMS),[3] Rutherford backward scattering(RBS)[4] and so on. However, there have been few studies to estimate interactions between superconducting oxides and various substrate materials quantitatively and to investigate the preparation conditions in order to obtain film with good quality.

In this chapter, physical and chemical interactions are investigated semi-quantitatively.[5-8] Thermal expansions of superconducting oxides and substrate materials were measured and the width of formed crack showed good agreement with the mismatch of thermal expansion between superconductor and substrate

materials. Chemical interaction was evaluated using powder mixture of superconductor and substrate materials by X-ray diffraction and ac-susceptibility measurement. MgO, $BaTiO_3$, $SrTiO_3$, YSZ, ZrO_2, Sus316, TiO_2, Al_2O_3, AlN, Si_3N_4, SiO_2, Si, WC, Cr_2O_3, MgF_2, CaF_2, SrF_2 and BaF_2 were examined as substrate materials.

3-2. Thermal expansion coefficients of High T_c Superconductors

3-2-1. Experimental

$(La_{0.9}Sr_{0.1})_2CuO_{4-\delta}$(LSCO), $Ba_2LnCu_3O_{7-\delta}$(BLnCO Ln=Y, Yb, Ho) and $BiSrCaCu_2O$(BSCCO) powders were prepared by mixing the prescribed amounts of oxides (CuO, Ln_2O_3, Bi_2O_3) and/or carbonates ($BaCO_3$, $La_2(CO_3)_3$) of component metals in ethanol and calcining the mixtures at 1000 ℃ for 16h in the case of LSCO, 900 ℃ for 12h in the case of BLnCO and 800 ℃ for 12h in the case of BSCCO. After being regrounded in an agate mortar, each powder was pressed at 900kg/cm^2 and sintered 20h at 1000 ℃ for LSCO, 20h at 940 ℃ for BYCO, 20h at 900 ℃ for BYbCO and 20h at 800 ℃ for BSCCO. The pellet was cut into rectangular specimens of 3x2x5mm^3. The specimens were then annealed at the temperatures described above for 20h and cooled in the furnace at a rate of about 0.5 ℃/min. X-ray diffraction measurement showed the presence of small amount of perovskite phase in the main LSCO phase, the single phase of BYCO, the presence of small amount of $BaCuO_2$ in the main BYbCO phase and the main so-called 80K phase of BSCCO. The sintering degree of the specimens were calculated to be 82~86% from the density of the specimens.

Thermal expansion coefficients of these samples and ceramic

substrates were measured in the temperature range of 30 °C through 900 °C by dilatometer (Sinku-Riko DL7000RH) whose push rod was fused silica. The measurement were carried out both in air and O_2 atmospheres. Heating and cooling rates mainly employed were 50 °C/min and 10 °C/min, respectively. In some cases a heating and cooling cycle at 3 °C/min was employed. Thermal expansion of substrate materials, MgO, $SrTiO_3$, YSZ (3mol% yttria stabilized zirconia), alumina, Corning #7059, quartz and sapphire were also measured.

3-2-2. Results and Discussion

Table 3-1 lists the mean thermal expansion coefficients of superconductor and substrate materials. Superconductors have expansion coefficients exceeding $1.2\times10^{-5}\,°C^{-1}$, exceptionally high as compared to the coefficients of easily available ceramics such as alumina and quartz. $SrTiO_3$, YSZ and MgO have close thermal expansion coefficients to those of superconducting oxides. In Fig. 3-3 is shown the crack observed in a scanning electron micrograph of LSCO film sputter-deposited on Corning #7059 glass substrate. Cracks about 0.04μm wide were formed in the film at about 10μm intervals when the film was annealed at 590 °C for 15h. According to Table 3-1, the mean linear expansion coefficient for LSCO is $1.44\times10^{-5}\,°C^{-1}$ and that for Corning #7059 is $0.50\times10^{-5}\,°C^{-1}$. Supposing that the cracks were formed by the difference in thermal expansion coefficient between the LSCO and Corning #7059, the width of crack is calculated as follows.

$$10\times(1.44\times10^{-5}-0.50\times10^{-5})\times(590-20)=0.054(\mu m)$$

This calculated value is consistent with the observed crack width. Thus, the thermal expansion coefficient is one of the most

significant factors in the choice of a substrate material in the preparation of superconducting films. Crack formation can be observed even in a BYbCO film sputter-deposited on $SrTiO_3$ and annealed in a furnace, although $SrTiO_3$ has only a slightly smaller mean thermal expansion coefficient than BYbCO.

Figure 3-4 shows relative expansion and the temperature dependences of thermal expansion coefficients of BYCO and BSCCO measured in air. Two bending points appear at about 350 °C and 650 °C in thermal expansion of BYCO, apparently corresponding oxygen uptake and seccession[9] and to the orthorombic-tetragonal phase transition,[10] respectively. On the other hand, such clear bending points were not observed in the thermal expansion of LSCO and BSCCO. Figure 3-5 compares the thermal expansion of BYCO determined in this work and those calculated as the cubic root of cell volumes elucidated by either neutron diffraction[11] or X-ray diffraction.[12] The data were almost parallel. The slight difference could be attributed to the existence of voids in the sintered specimens used in this study. The data calculated from cell volumes correspond to single crystal specimens. The diffraction data indicate that the thermal expansion parallel to the c-axis is larger than that perpendicular to the c-axis. Based on the I-V curve measured on a single-crystal BYCO film deposited on $SrTiO_3$ (110) substrate, Enomoto and coworkers suggested the formation of microcracks along c-axis.[13]

3-2-3 Conclusion

(1) Thermal expansion coefficients of high-T_c superconductor oxides are larger than those of ceramics which are conventionally

used as substrates. Therefore, the use of substrates which have relatively large thermal expansion coefficient (YSZ, $SrTiO_3$ and MgO for example) is recommended for film deposition.

(2) By examining the dependence of thermal expansion coefficients on temperature, information such as change of oxygen content and phase transition can be obtained.

3-3. Chemical Interaction between Superconductor and Substrate Materials in Solid State

3-3-1. Experimental

Figure 3-6 depicts the flow chart of experimental procedure for evaluating the chemical interaction. Substrate materials examined were powdery $SrTiO_3$, $BaTiO_3$, MgO, ZrO_2, GGG(gallium gadorinium garnet), quartz, TiO_2, YSZ(yttria stabilized zirconia), Al_2O_3, amorphous silica, MgO, CaF_2, SrF_2, BaF_2, AlN, Si_3N_4, sus 316, WC and Cr_2O_3. Average size of these powders were 4-6μm. These powders were dried in vacuo at 150°C or 200°C for 1h to remove adsorbed moisture. $Ba_2LnCu_3O_{7-\delta}$(BLnCO: Ln=Yb, Y, Gd) powder was prepared by calcining the nominal amount of mixture of $BaCO_3$, Ln_2O_3 (Ln=Yb, Y, Gd) and CuO at 900 ℃ for 9h and 910°C for 24h followed by slow cooling at a rate of 1 °C/min. Powdery $Bi_2Sr_2CaCu_2O_x$(BSCCO) was prepared by calcining the nominal amount of mixture of Bi_2O_3, $SrCO_3$, $CaCO_3$ and CuO at 800°C for 10h followed by the heat-treatment at 830°C for 5h. BLnCO and BSCCO were confirmed to be 90K-class and 80K-class superconductors, respectively, from ac-susceptibility measurement. X-ray diffraction measurement (MAC Science MXP^3) showed that BYCO, BGdCO and BSCCO were single phase and BYbCO contained small amount of $BaCuO_2$. Average size of these superconducting powders

were 2~6μm.

Mixtures of 80vol.% of superconductor and 20vol.% of substrate materials were heated at 600°C, 700°C, 800°C and 900°C for 2h either in air or in dry Ar (80%) and O_2(20%) mixed gas. The reaction products were characterized by X-ray diffraction measurement. The relative volume fraction of superconductivity was estimated from the ac-susceptibility at 1kHz measured from the change of inductance of the coil which was wound around a sample tube. The TG-DTA of the mixtures was measured to estimate the temperatures of solid phase reaction and impurity adsorption by using an MAC TG-DTA2010.

3-3-2. Results and Discussion

3-3-2-1 Chemical Reactivity of BYCO with Various Substrate Materials

Figure 3-7(a) shows the temperature dependence of ac-susceptibility measured for a mixture of BYCO and amorphous SiO_2 after being heated at various temperatures. In order to semi-quantitatively evaluate the deterioration of superconducting BYCO, a normalized relative volume fraction was defined by dividing the value of dL/W(μH/g) at 4.2K of the heat-treated mixture by that of the mixture prior to the heat-treatment (Fig. 3-7(b)), where dL and W are the values of ac-susceptibility and the weight of the sample respectively.

Figure 3-8 shows the same evaluation made for the mixtures of BYCO and the other substrate materials. Substrate materials roughly be divided into 4 groups depending on the temperature at which the relative volume fraction decreases below 75%. The

relative volume fraction for the mixture of BYCO and either $SrTiO_3$ or MgO was higher than 75% even after a 900°C heat-treatment for 2h. The heat-treatment at 900°C made the relative volume fractions for the mixtures of BYCO and YSZ, ZrO_2, Al_2O_3, TiO_2 and SUS316 less than 75%, although they were preserved to be higher than 75% after the heat-treatment at 800°C and below. The relative volume fraction for the mixture of BYCO and either amorphous SiO_2 or Si decreased below 75% at 800°C. The heat-treatment at 600°C reduced the relative volume fraction below 75% for the mixture of BYCO and either one of CaF_2, WC or Cr_2O_3.

X-ray diffraction analysis of the heat-treated mixtures identified such reaction products as listed in Table 3-2, in addition to the unreacted BYCO. The result indicates that barium in BYCO is likely reactive with metallic components of substrate materials; the heat-treatment generally produced oxides composed barium and components of substrate materials.

3-3-2-2 Chemical Reactivity of BLnCO with Oxides and Nitrides

Figure 3-9 shows the relative superconductor volume fraction for the mixtures of BLnCO and various oxide substrate materials heat-treated at 800°C. Relative volume fractions ranged between 75% and 100% without any significant change depending on the lanthanide species. Compared to these oxides, nitride substrate materials showed higher reactivity with BLnCO as shown in Fig. 3-10. Among the three BLnCO superconductors (Ln=Yb, Y, Gd) examined, BGdCO had the lowest reactivity.

Table 3-3 lists the reaction products detected by XRD analysis for the mixtures of BYCO and substrate materials. The same Ba containing oxides were observed as the products in the

reactions with both oxides and nitrides.

3-3-2-3 Reactivity of BLnCO and BSCCO with Alkaline Earth Fluorides

The heat-treatment at a temperature as low as 600°C in air reduced not only relative superconducting volume fraction but also $T_{c,\,onset}$ of the mixture of BYCO and CaF_2 as Fig. 3-11 shows. Decreases of critical temperature by heat treatment in air as low as 600°C were also observed for the mixtures of BYCO and MgF_2, SrF_2 and BaF_2. Figure 3-12 shows the variation of $T_{c,onset}$ for a mixture of BYCO and MF_2 (M=Ca, Sr, Ba) by the heat-treatment at various temperature in air. On the contrary, $T_{c,\,onset}$ values of mixtures of BSCCO and MF_2 were unchanged by the heat-treatment under the same conditions(see Fig. 3-13). It was, however, premature to conclude that BYCO is more reactive to MF_2 than BSCCO. Komatsu and coworkers reported that BYCO was inert to BaF_2 for the heating of discs composed of BYCO and BaF_2 at 900°C for 24h.[14)]

Figure 3-14 shows the TG-DTA measurement for a mixture of BSCCO and CaF_2. An endothermic peak accompanied by a small weight loss was observed at 175°C, suggesting the existence of moisture which adsorbed so strongly to CaF_2 that it had not been removed by drying in vacuo at 150°C. The endothermic peak at 175°C was also observed in pure MF_2 powders dried at 150°C. Alternatively, BYCO may be deteriorated either with water,[15)] which could be present in air, or which with a hydrolyzed product of CaF_2 with the water. To avoid the influence of this adsorbed moisture or contaminated water in air, MF_2 powders were dried in vacuo at

200°C, mixed with the superconducting oxide and heated in an atmosphere of dry Ar(80%) and O_2 mixed gas. Figure 3-15 shows the temperature dependence of ac-susceptibility for this heated mixture of CaF_2 and BYCO. Here, the mixture did not change its $T_{c,\ onset}$ of 92K after heat-treatments both at 600°C and 800°C, although the ac-susceptibility decreased to some extent. When the heat-treatment at 600°C was done in air, the mixture reduced its $T_{c,\ onset}$ to 80K. This reduction of $T_{c,\ onset}$ is obviously ascribed to the moisture in air. Such reduction of $T_{c,\ onset}$ was not observed for the mixtures of MF_2 and BSCCO, thus reinforcing the observation that BSCCO has a higher endurance than BYCO against moisture.

Figure 3-16 shows the variation of relative superconducting volume fractions for the mixtures of BYCO and MF_2 after heat treatment in the dry atmosphere. Due to the heat treatment at 800°C, the volume fraction for the mixture of BaF_2 and BYCO decreased to 82% of that the preheated mixture. This value is, however, only slightly lower than the 88% obtained for the mixture of MgO and BYCO and far higher than the relative volume fraction (42%) obtained after heat treatment in air. Heat treatment in air induced a significant decrease similarly for the mixture BYCO with CaF_2 and SrF_2. Even in the dry atmosphere, the volume fraction for the CaF_2-BYCO mixture greatly decreased, especially after heat treatment at 700°C and higher. By the XRD analysis, BaF_2 was detected as the main reaction product for the heat-treated mixtures of MF_2 (M=Ca, Sr) and BYCO. Presumably, fluorine in MF_2 extracted Ba from BYCO. From the free energy of formation,[16] BaF_2 is the most stable among these alkaline earth

fluorides and oxides. Due to the lack of thermodynamical data for BYCO, the change of Gibbs free energies (ΔG) for the reactions of $BaO+MF_2 \rightarrow MO+BaF_2$ (M=Ca, Sr, Ba) were calculated instead of those for the reactions between MF_2 and BYCO. Assuming that enthalpy and entropy are independent on temperature, ΔG values at 800 C are -68, -28 and 0kJ/mol for the reactions of M=Ca, Sr and Ba, respectively, in good agreement with order of chemical reactivity of these fluorides.

The chemical reactivity of MF_2 with BSCCO was different from that of MF_2 and BYCO. The order of the chemical reactivity of MF_2 to BSCCO was $SrF_2 < CaF_2 < BaF_2$ as Fig. 3-17 shows. More than 90% of the superconducting volume fraction was maintained for the mixture of CaF_2 or SrF_2 after a 700°C heat treatment. By the X-ray diffraction measurement, SrF_2 was detected as a reaction product in the heated mixture of BaF_2 and BSCCO. BaF_2 was not detected as a reaction product in the heated mixture of BSCCO and other alkaline earth fluorides, but peaks of some unidetified reaction products were detected instead by X-ray diffraction.

3-3-2-4 Chemical Interaction between BSCCO and Substrate Materials

Table 3-4 gives the relative superconductor volume fraction in the mixtures of BSCCO and substrate materials heated at 800°C. Substrate materials can be classified into three groups with their relative volume fraction of >95%, 85~50%, and <25%, respectively. More than 100% volume fractions were obtained for some mixtures presumably because the heat-treatment promoted further sintering of BSCCO rather than a solid state reaction

between BSCCO and the substrate materials.

From the viewpoint of reactivity, GGG is considered to be a promising substrate material. A mixture of GGG and BSCCO gave volume fraction of 105% after the 800°C heat-treatment. ZrO_2 and YSZ(yttria stabilized zirconia) appeared to be largely different in the reactivity. Figure 3-18 depicts a TG-DTA curve for the mixture of BSCCO and ZrO_2. An endothermic peak due to the melting of BSCCO was observed at about 880°C and any other peak suggesting a solid phase reaction was not observed. On the other hand, peak corresponding to a solid phase reaction was observed in DTA curve of the mixture of BSCCO and YSZ at 804°C(Fig. 3-19). From XRD analysis, $SrZrO_3$ was detected as a reaction product in the mixture of BSCCO and YSZ but it was not in the mixture of BSCCO and ZrO_2. This result indicates yttrium enhances a chemical reaction between ZrO_2 and BSCCO. Fukushima and coworkers reported that yttrium could substitute the Ca-site in BSCCO by the heat-treatment at 920°C.[17)]

3-3-3. Conclusion

It is verified that $SrTiO_3$ and MgO had low reactivity with superconductors. Alkaline earth fluorides in superconductors are easily react with substrate materials.

3-4. General Conclusion

Physical and chemical interactions between superconducting oxides and substrate materials were evaluated semi-quantitatively. MgO and $SrTiO_3$ were suitable substrate materials to prepare superconducting films. In order to use other materials as substrate, low temperature synthesis below 600°C would be required to avoid crack formation and solid phase reaction.

References

1) H. Koinuma, M. Kawasaki, T. Hashimoto, S. Nagata, K. Kitazawa, K. Fueki, K. Masubuchi and M. Kudo: Jpn. J. Appl. Phys., 26 (1987) L763.

2) H. Nagata, A. Takano, M. Kawasaki, M. Yoshimoto and H. Koinuma: J. Am. Ceram. Soc., 72 (1989) 680.

3) For example, J. Chang, M. Matsui, M. Iwase and S. Kashiwa: Extended Abstract of the 35th Spring Meeting of The Japan Society of Applied Physics and Related Societies (1988) 109.

4) H. Nakajima, S. Yamaguchi, K. Iwasaki, H. Morita and H. Fujimori: Appl. Phys. Lett., 53 (1988) 1437.

5) T. Hashimoto, K. Fueki, A. Kishi, T. Azumi and H. Koinuma: Jpn. J. Appl. Phys., 27 (1988) L214.

6) H. Koinuma, T. Hashimoto, M. Kawasaki, K. Kitazawa, K. Fueki, A. Inoue and Y. Okabe: the Proc. of SPIE vol.948 High-T_c Superconductivity: Thin Films and Devices (1988) 25.

7) H. Koinuma, K. Fukuda, T. Hashimoto and K. Fueki: Jpn. J. Appl. Phys.,27 (1988) L1216.

8) T. Hashimoto, T. Yoshida, M. Yoshimoto, M. Takata and H. Koinuma: Rep. of the Res. Lab. of Eng. Mater., Tokyo Inst. of Tech., 14 (1989) 91.

9) K. Kishio, J. Shimoyama, T. Hasegawa, K. Kitazawa and K. Fueki: Jpn. J. Appl. Phys., 26 (1987) L1228.

10) K. Yukino, T. Sato, S. Ooba, M. Ohta, F. P. Okamura and A. Ono: Jpn. J. Appl. Phys., 26 (1987) L869.

11) J. D. Jorgensen, M. A. Beno, D. G. Hinks, L. Soderholm, K. J. Vollin, R. L. Hitterman, J. D. Grace, I. K. Schuller, C. U.

Serge, K. Zhang and M. S. Kleefisch: Phys. Rev., B36 (1987) 3608.

12) H. M. O'Bryan and P. K. Gallagher: Adv. Cer. Mater. 2, special issue (1987) 640.

13) Y. Enomoto, T. Murakami, M. Suzuki and K. Moriwaki: Jpn. J. Appl. Phys., 26 (1987) L1248.

14) T. Komatsu, O. Tanaka, K. Matusita and T. Yamashita: Jpn. J. Appl. Phys., 27 (1988) L1686.

15) M. F. Yan, R. L. Barns, H. M. O'Brian, Jr., P. K. Gallagher, R. C. Sherwood and S. Jin: Appl. Phys. Lett., 51 (1987) 532.

16) O. Kubaschewski and C. B. Alcock: Metallurgical Thermochemistry (Pergamon Press, Oxford, 1979) 5th ed.

17) N. Fukushima, H. Niu and K. Ando: Jpn. J. Appl. Phys., 27 (1988) L790.

Fig. 3-1. Scanning electron micrograph of LSCO films prepared by ac 50Hz sputtering and annealed at 590°C for 15h. (substrate: Corning #7059 glass)

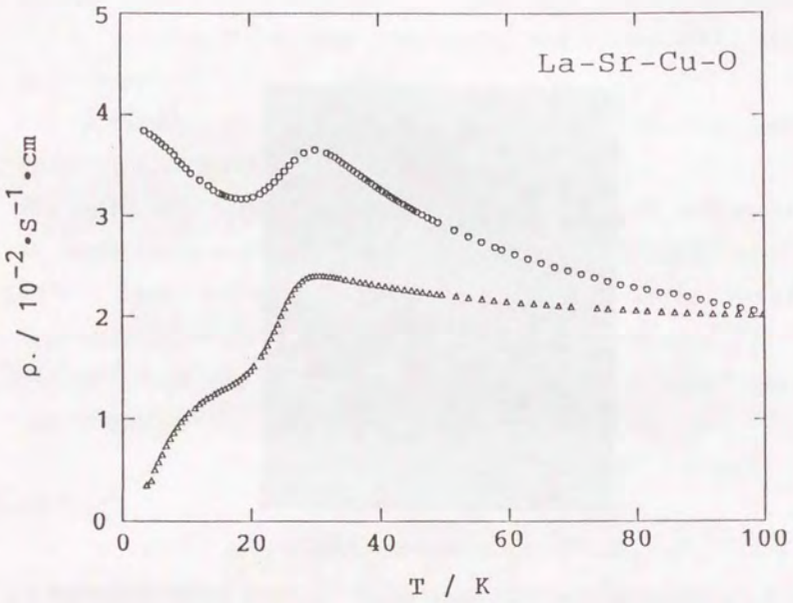

Fig. 3-2. Resistivity vs. temperature relationships for LSCO films sputter-deposited on Corning #7059 glass and subsequently annealed at 580 °C for 50h (○) and at 585 °C for 15h (△) in O_2.

Table 3-1. Mean thermal expansion coefficients of superconductor and representative substrate materials.

Materials		Mean thermal expansion coefficient (10^{-5} °C^{-1})	
		30~500°C	30~900°C
superconductor	$(La_{0.9}Sr_{0.1})_2CuO_{4-\delta}$	1.44	1.38
	$Ba_2YCu_3O_{7-\delta}$	1.44	1.69
	$Ba_2YbCu_3O_{7-\delta}$	1.27	1.50
	$Bi_1Sr_1Ca_1Cu_2O_x$	1.20	1.35
substrate	$SrTiO_3$	1.02	1.11
	YSZ	1.00	1.03
	MgO	1.24	1.30
	sapphire	0.68	0.75
	alumina	0.62	0.70
	#7059 glass	0.50	-
	quartz	<0.1	<0.1

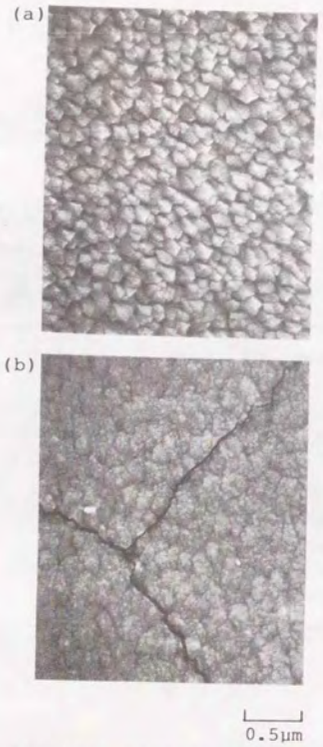

Fig. 3-3. Scanning electron micrographs of LSCO surface deposited on Corning #7059 glass. a) as-deposited, b) after annealing at 590 °C for 15h.

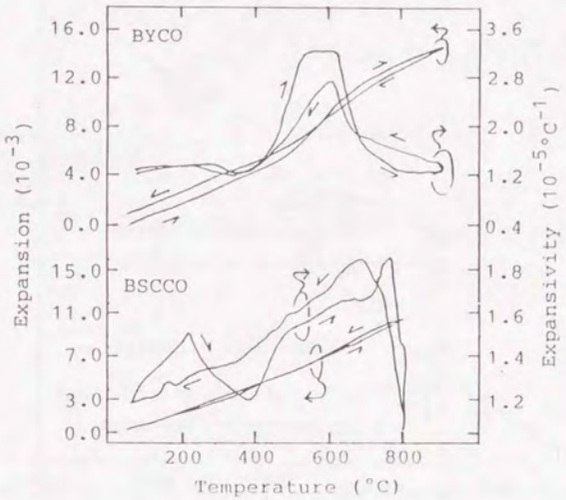

Fig. 3-4. Thermal expansion behavior of BYCO and BSCCO in air. Heating rate: 50°C/min, cooling rate: 10°C/min.

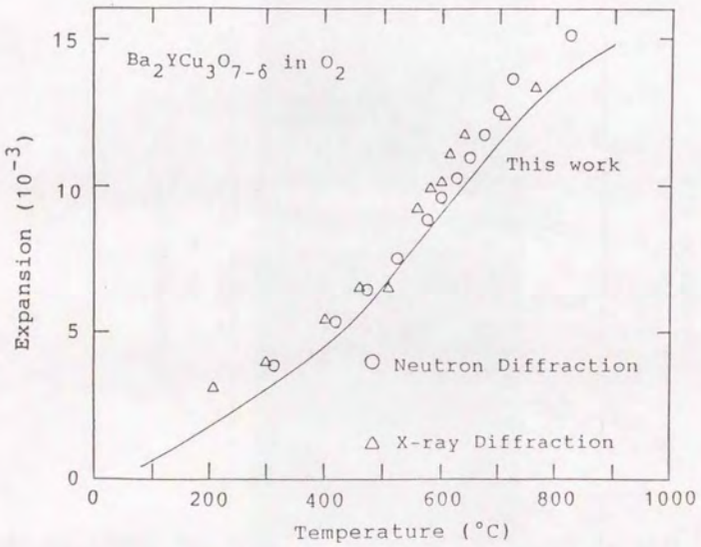

Fig. 3-5. Comparison of temperature-dependent thermal expansions determined for BYCO in O_2 atmosphere by various methods.

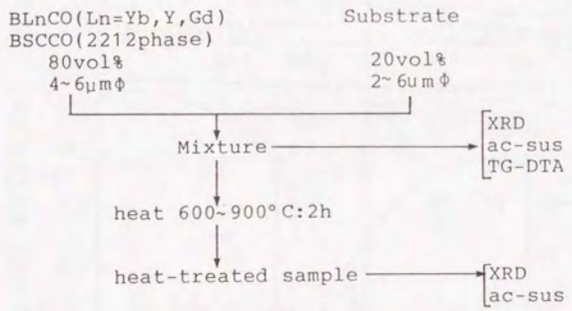

Fig. 3-6 Experimental flow chart for the evaluation of chemical reactivity of superconducting oxide with substrate materials.

Volume fraction (%)

=dL/W after heating (4K)/dL/W before heating (4K)

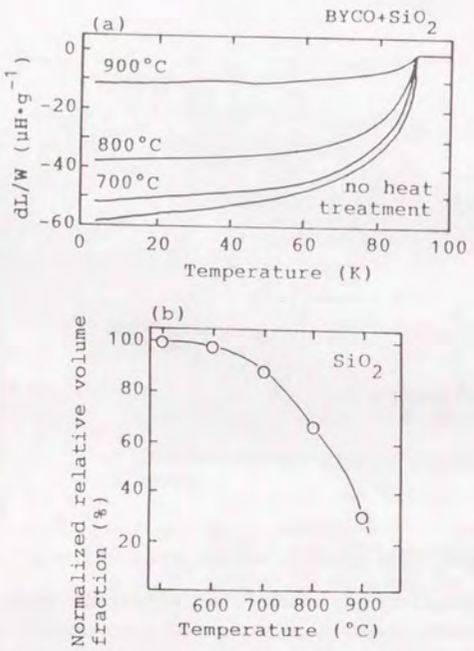

Fig. 3-7. (a)Temperature dependence of ac-susceptibility for a heat-treated mixture of BYCO and amorphous SiO_2 at various temperatures. (b) Variation of the relative volume fraction of superconductivity at 4.2K for a mixture of BYCO and amorphous SiO_2 by the heat-treatment at various temperatures.

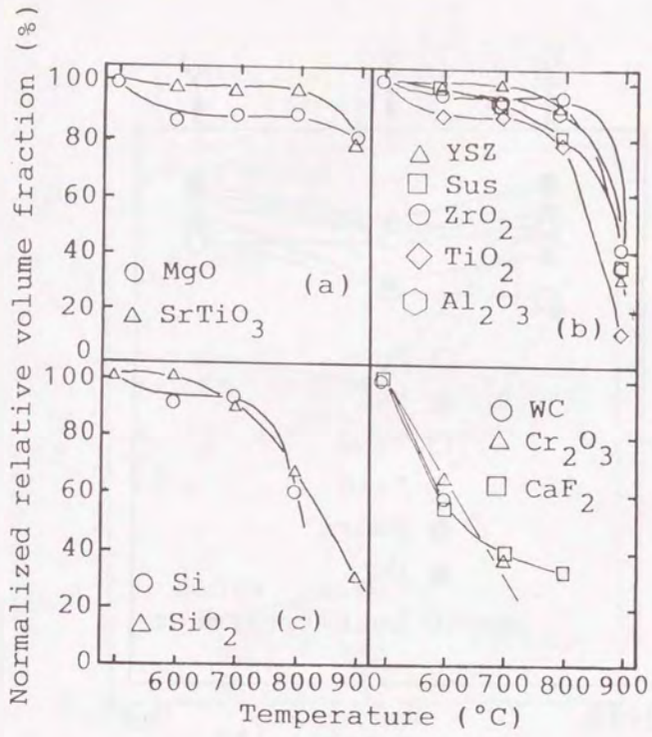

Fig. 3-8. Variation of the volume fraction of superconductivity at 4.2K for the mixtures of BYCO and various substrate materials by 2h heat-treatment at temperatures ranging from 600°C to 900°C.

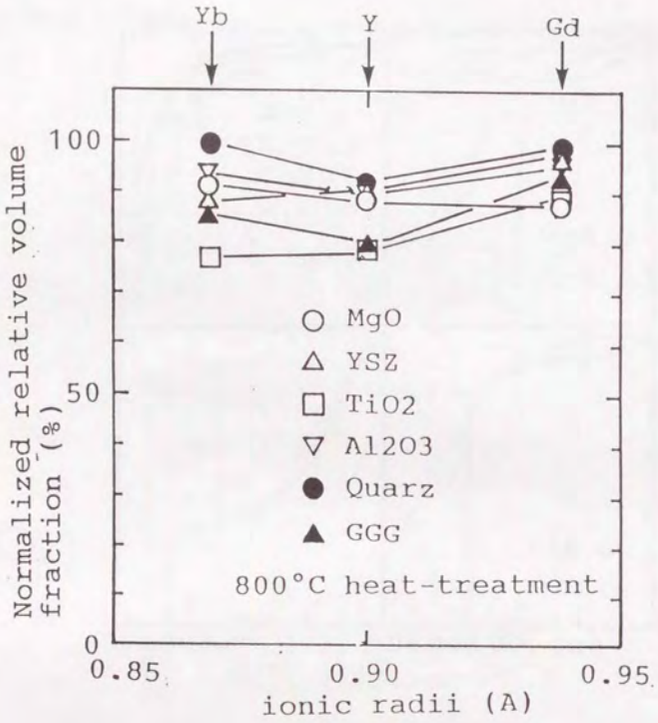

Fig. 3-9. Relative volume fraction of superconductor for the mixtures of BLnCO and oxide substrate materials heated at 800 ℃ for 2h.

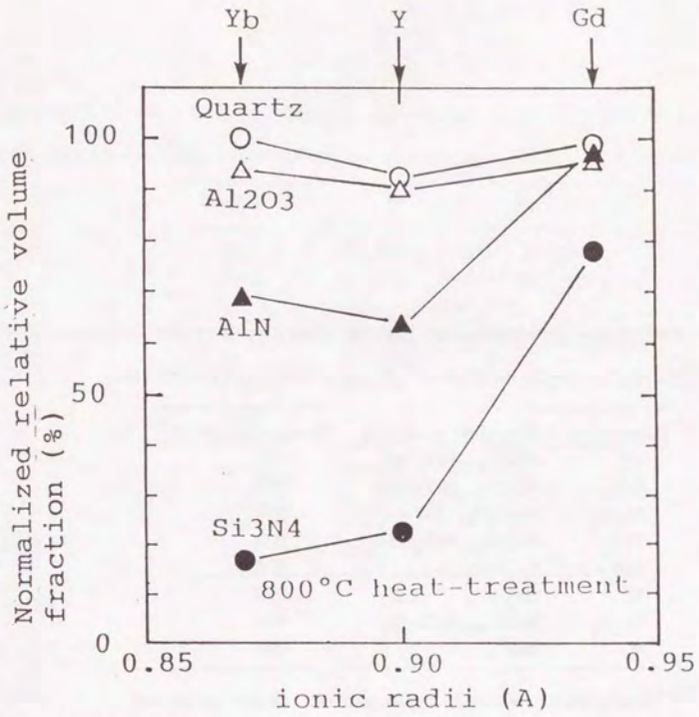

Fig. 3-10. Relative volume fraction of superconductor for the 800 C heat-treated mixtures of BLnCO and AlN and Si_3N_4. Fraction of 800 °C heat-treated mixture of BLnCO and Al_2O_3 and quartz are shown for comparison.

Table 3-2. Reaction products of solid state reaction between BYCO and substrate materials detected from X-ray diffraction.

Substrate	Reaction products	Temperature(°C)*
YSZ	$BaZrO_3$, BaY_2CuO_5	900
ZrO_2	$BaZrO_3$, BaY_2CuO_5	900
Al_2O_3	$BaAl_2O_4$, BaY_2CuO_5	900
TiO_2	$BaTiO_3$, BaY_2CuO_5	800
SiO_2	Ba_2SiO_4	800
Si	Ba_2SiO_4	700
Cr_2O_3	$BaCrO_4$, $BaCr_2O_4$	600
WC	$BaWO_4$	600

*Temperature of heat treatment at which reaction products were detected by X-ray diffraction measurement.

Table 3-3. Reaction products of solid state reaction b-tween BYCO and oxide and nitride used as substrate.

Substrate	Reaction Product
YSZ	$Ba_3Zr_2O_7$ $BaZrO_3$ BaY_2CuO_x
ZrO_2	$Ba_3Zr_2O_7$ $BaZrO_3$ BaY_2CuO_x
Al_2O_3	$BaAl_2O_4$ BaY_2CuO_x
AlN	$BaAl_2O_4$ BaY_2CuO_x
Si	Ba_2SiO_4
a-SiO_2	Ba_2SiO_4
Si_3N_4	Ba_2SiO_4
TiO_2	$BaTiO_3$ BaY_2CuO_x
$BaTiO_3$	$BaCuO_2$ BaY_2CuO_x
$SrTiO_3$	$BaCuO_2$(?)BaY_2CuO_x(?)
MgF_2	BaF_2
CaF_2	BaF_2

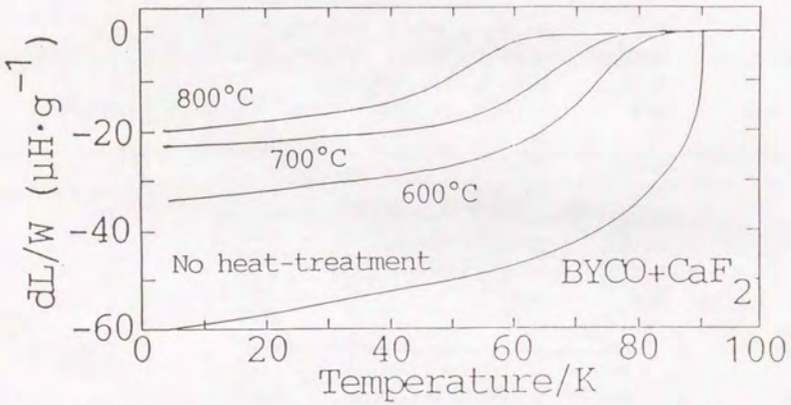

Fig. 3-11. Temperature dependence of ac-susceptibility for a mixture of BYCO and CaF_2 measured after heat treatment at various temperatures for 2h. CaF_2 was dried in vacuo at 150 °C for 1h.

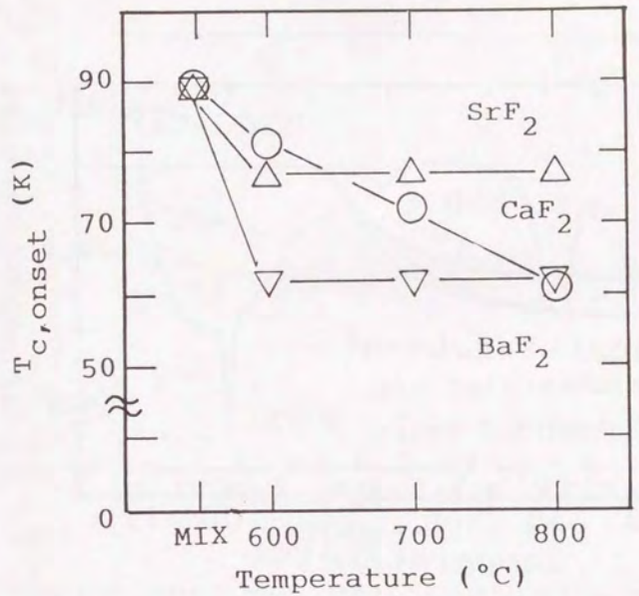

Fig. 3-12. Variation in $T_{c,\ onset}$ for BYCO-MF_2 mixtures by the heat-treatment in air at 600 °C, 700 °C, and 800 °C.

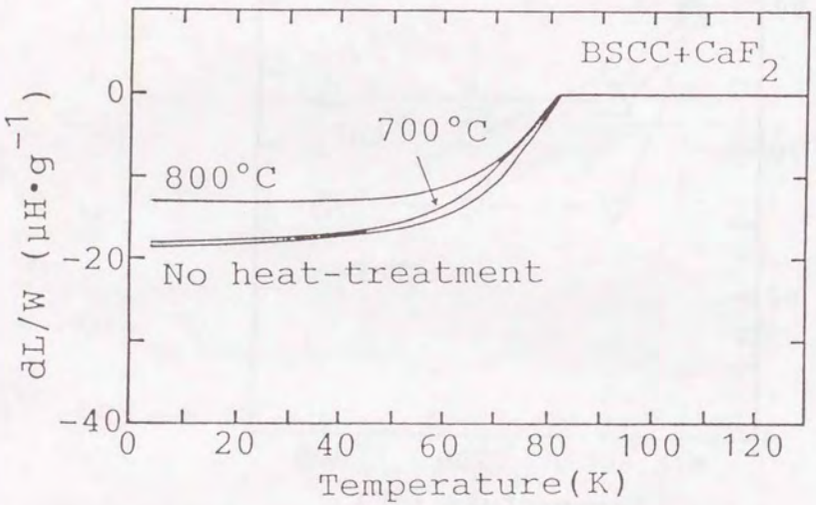

Fig. 3-13. Temperature dependence of ac-susceptibility for heated and unheated mixtures of BSCCO and CaF_2 powders. The heating was carried out in air.

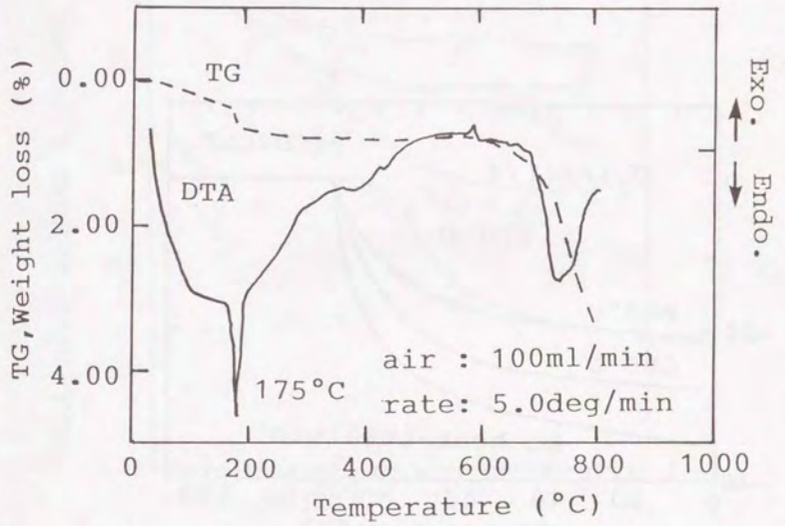

Fig. 3-14. TG-DTA measurement for a mixture of CaF_2 (20vol%) and BSCCO(80vol%).

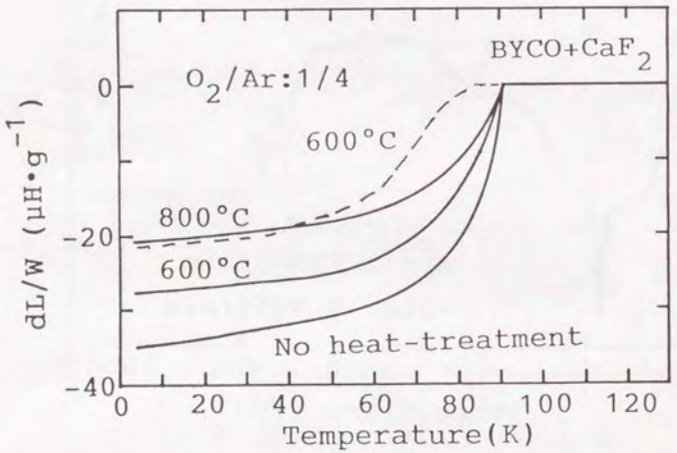

Fig. 3-15. Dependence of ac susceptibility on temperature for mixtures of BYCO and CaF_2 heat treated at temperatures of 600°C and 800°C, The CaF_2 was dried in vacuo at 200°C before mixing. The solid and dashed lines are for heating in dry Ar(80%) and O_2(20%) mixed gas atmosphere and in air, respectively.

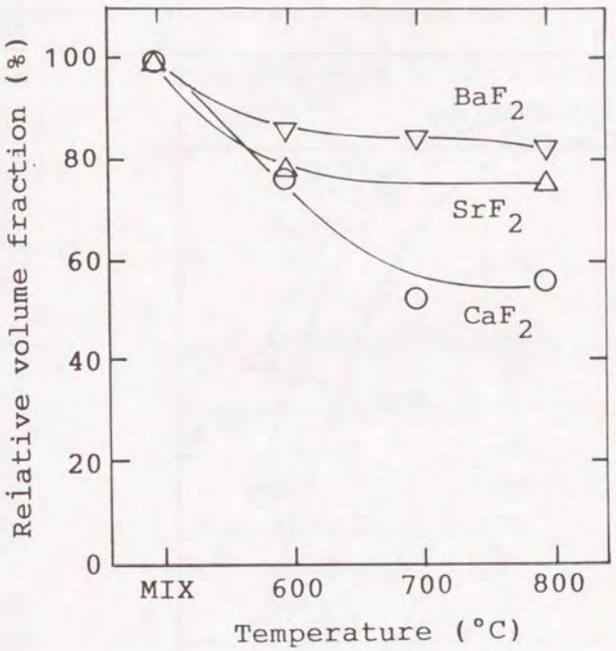

Fig. 3-16. Variation of relative superconducting volume fractions at 4.2K for the mixtures of MF_2 and BYCO resulting from heat treatment. MF_2 was dried in vacuo at 200°C in advance and heat treatment was performed under an atmosphere of dry Ar(80%) and O_2(20%) mixed gas.

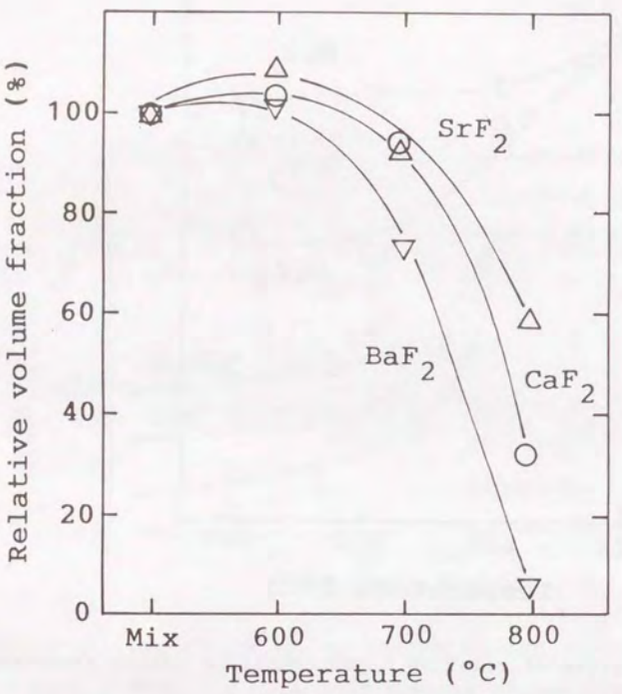

Fig. 3-17. Relationship between heat-treatment temperature and relative volume fraction of the superconductor of MF_2 and BSCCO. The heat treatment was carried out under dry Ar(80%) and O_2(20%) mixed gas.

Table 3-4. Relative volume fractions of the mixture of BSCCO and various substrate materials heated at 800°C.

Group	Substrate	Volume fraction at 800°C (%)
A	$SrTiO_3$	120
	MgO	110
	ZrO_2	110
	GGG	105
	Quartz	99
	TiO_2	96
B	sus316	85
	CaF_2	80
	Al_2O_3	74
	a-SiO_2	71
	BaF_2	51
C	YSZ	22
	Si	14
	AlN	11
	Si_3N_4	8

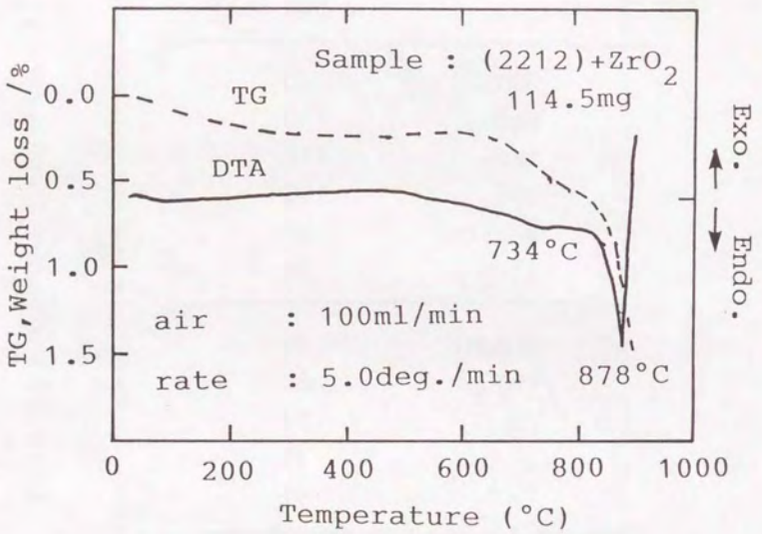

Fig. 3-18. TG-DTA curves for a mixture of BSCCO and ZrO_2.

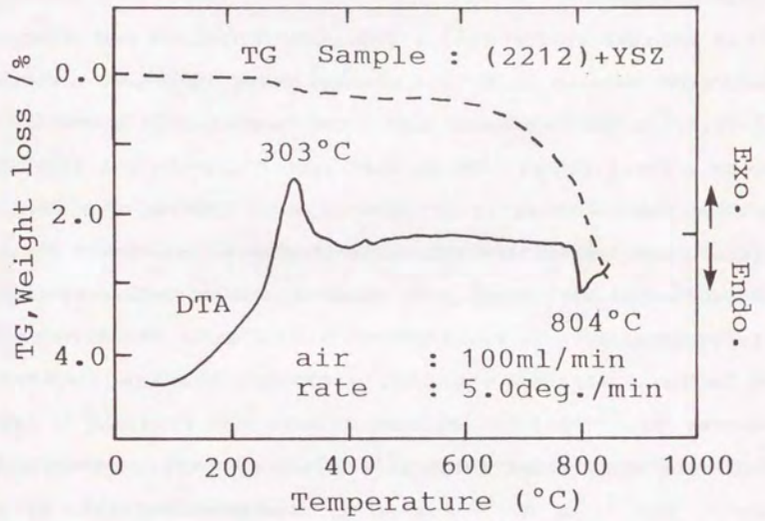

Fig. 3-19. TG-DTA curves for a mixture of BSCCO and YSZ.

Chapter 4

Preparation of Oxide Films Relating to High-T_c Superconductor at Low Temperature by Plasma CVD

4-1. Introduction

In chapter 3, the author indicated physical and chemical interaction between high-T_c superconducting film and substrate materials. It was concluded that low temperature (below 600°C) process without interaction between superconductor and substrate was required in order to prepare film of desired quality. In addition, low temperature process will also be necessary for the construction of artificially designed crystal structure by layer-by-layer deposition to avoid interdiffusion among the layers.

So far, various methods, such as activated reactive evaporation,[1] plasma assisted laser ablation,[2] light irradiation during sputtering,[3] molecular beam epitaxy using ozone[4], N_2O[5], or NO_2[6] and so on have been reported as low temperature processes. Fabrication of multilayered films by laser ablation,[7] sputtering,[8-10], and molecular beam epitaxy[11] have also been reported. Besides these physical vapor deposition(PVD), chemical vapor deposition (CVD) can also be a low temperature process. Figure 4-1 shows schematic energy diagrams of PVD and CVD. In case of CVD, low temperature sinthesis of a film can be expected by utilizing chemical energies of sources and electrochemical excitation by plasma or photon. Moreover, CVD is suitable for the fabrication of oxide films because film growth can be carried out under higher oxygen atmosphere than PVD.[12] In addition, CVD has been expected to be a process for layer-by-layer deposition due to its higher controllability than PVD.

Although CVD's of high-T_c superconductor have already been reported by several groups,[13-19] most of them employed thermal CVD using substrate temperatures higher than 700°C. Decrease of substrate temperature to 570°C using plasma has been reported by Kanehori et. al.,[15] Zhao et. al.,[16] and Kobayashi et al.,[17] however, they introduced source materials simultaneously and there have been few reports on the synthesis of multilayered film by CVD.

As a fundamental study toward the artificial construction of layered structure, low temperature CVD's of oxide films relating to Bi-Sr-Ca-Cu-O superconductor using microwave plasma[18] and rf glow-discharge plasma[19] from each one of the sources were presented in this chapter. Constant deposition rates were obtained by using some sources examined.

4-2. Microwave Plasma CVD of Oxide Films Relating to High-T_c Bi-Sr-Ca-Cu-O Superconductor

4-2-1. Experimental

In Fig. 4-2, structures of CVD sources used in the study are depicted. They were reported to have moderate high vapor pressures below 240°C.[20] In the case of microwave plasma CVD, sources used were $Bi(C_6H_5)_3$, $Sr(PPM)_2$, $Ca(PPM)_2$, and $Cu(HFA)_2$. These sources supplied from Tri-Chemical Co., Ltd. and/or purchased from Ube-kosan Co., Ltd. were separately heated in oil baths and carried into the reaction chamber with helium at a total pressure of 100Torr. The evaporation temperatures were determined in view of the TG data (Fig. 4-3) of the sources measured under Ar 100Torr atmosphere using a Sinku-Riko model

TGD-7000RH. To avoid the condensation of source materials, the gas lines were heated at a temperature above the highest oil bath temperature. Figure 4-4 shows schematically the microwave CVD apparatus used in this study. A 2.45GHz microwave was applied to either a quartz tubing for Ar flow or a double quartz tubing, inner and outer for the introduction of Ar and O_2 gases, respectively, to generate the Ar (and oxygen) plasma. The evaporated source materials encounter with the plasma above the substrate to be decomposed and oxidated efficiently. The substrates, MgO(100), Si(111), Si(100), and GaAs(100) were heated at a temperature between 200°C and 600°C by a focused IR lamp. The film thickness was measured by the stylus method using a Taylor-Hobson Talystep. The crystal structure and composition of the deposited films were analyzed by X-ray diffractometry (XRD: MAC Science MXP^3) and X-ray photo electron spectroscopy (XPS: JEOL-JPS80), respectively.

4-2-2. Results and Discussion

4-2-2-1. Preparation of CuO Film from $Cu(HFA)_2$

$Cu(HFA)_2$ was heated in an oil bath at 80°C and carried int the chamber in a stream of 80sccm He. The reaction pressure and microwave power were 1.5Torr and 90W, respectively. The crystal structure and composition of the films were highly dependent on the way of oxygen introduction to the reactor. Figure 4-5 depicts XPS spectra of Cu_{2p} of the film prepared at a substrate temperature of 600 °C on MgO(100). When the Ar and oxygen tubings were placed separately and away farther than 3cm from each other, only metallic Cu peaks were observed in the XPS of the deposited film. Satellite peaks which indicates the existence of divalent

Cu appeared when the distance between the oxygen and Ar outlet came closer to 0.5cm. Hence, we employed a double quartz tubing to supply more excited oxygen above the substrate so that the decomposed fragments could be oxidized effectively. Figure 4-6 shows XRD patterns of the films on MgO(100) prepared at 400°C at various O_2/Ar ratios. The crystal structure of the film was amorphous at an O_2/Ar ratio of 5sccm/50sccm. The peaks of both CuF_2 and CuO were detected by increasing the O_2/Ar ratio to 10sccm/50sccm. Increase in the O_2/Ar ratio to 15sccm/50sccm increased the intensities of CuO peaks and decreased those of CuF_2.

4-2-2-2. Preparation of Bi_2O_3 Film from $Bi(C_6H_5)_3$

The evaporation temperature of $Bi(C_6H_5)_3$ was determined to be 120°C because the weight decrease due to the sublimation started at about this temperature. The flow rate of He carrier gas, reaction pressure, and O_2/Ar ratio were set at 80sccm, 1.5Torr, and 10sccm/50sccm, respectively. Figure 4-7 shows the XRD patterns of the films prepared from $Bi(C_6H_5)_3$ on MgO(100) substrate at a temperature of 200°C. The microwave plasma power was 60W or 90W. When 60W microwave was applied, the obtained film was amorphous. The film prepared at microwave power of 90W showed XRD peaks all of which could be identified to be β-Bi_2O_3. Increase in the amount of excited oxygen species is considered to work effectively for the formation of crystalline oxide film. As Fig. 4-8 shows, the deposition rate was constant at 0.56A/s throughout the reaction time of 60min to give a film of 2000A thick. Carbon contamination in the film was not observed by XPS

measurement. The deposition temperature (200 °C) was lower than that (300 °C) reported by Okada et. al. for thermal CVD of Bi_2O_3 using $Bi(C_2H_5)_3$ as a source material.[21)]

4-2-2-3. Preparation of Oriented CaF_2 and SrF_2 Films

From the TG analysis, the evaporation temperature of $Sr(PPM)_2$ and $Ca(PPM)_2$ were determined to be 240°C and 200°C, respectively. Flow rate of He, Ar, and O_2 were 80, 50, and 10sccm, respectively. The substrate temperature and reaction pressure were 400°C and 1.5Torr. The microwave power was 90W. Figure 4-9 shows XRD patterns of the films prepared on MgO(100) substrate. The CaF_2 and SrF_2 films strongly oriented to (001) direction were prepared from $Ca(PPM)_2$ and $Sr(PPM)_2$, respectively. The orientation of CaF_2 film could be controlled by the substrate as Fig. 4-10 shows. Films oriented to (001) were obtained on Si(100) and GaAs(100), while (111) oriented film was on Si(111) substrate. Rocking curves of (222) peak of CaF_2 film on Si(111) substrate are shown in Fig. 4-11. With the decrease in the film deposition rate from 3.6A/s to 1.3A/s, FWHM of the curves decreased from 0.45 to 0.28, which was close to 0.17 reported for the film epitaxially grown by MBE at 800°C.[22)] XPS measurement indicated that the Ca/F composition ratio was 0.4~0.5 and there was a little carbon and oxygen contamination on the film. These results suggest that this microwave plasma CVD is a promising new method for the heteroepitaxial CaF_2 and SrF_2 film deposition on semiconductor substrates such as Si and GaAs, at such a low temperature as 400 °C. Further optimization of reaction conditions including more careful cleaning of the substrate surface should decrease the carbon contamination and improve the crystal quality

of CaF_2 and SrF_2 films to such an extent that they could be used as a buffer layer between superconductor and semiconductor.

4-2-2-4. Synthesis of Superconducting Film by Annealing Layered Film

A layered film was prepared by successive deposition of Bi_2O_3, SrF_2, CaF_2, and CuO films of about 2000A each. Annealing the film at 850 °C for 30min in air yielded a $T_{c,\ onset}$ at 65K as shown in Fig. 4-12. However zero resistivity was not achieved. The interdiffusion required for the construction of superconducting phase should be difficult between such thick layers. Accumulation of thinner layers would facilitate the preparation of superconducting films at a low temperature.

4-2-3. Conclusion

As-grown Bi_2O_3, SrF_2, CaF_2, and CuO films were obtained at 400 °C or below by using a microwave plasma CVD apparatus. Superconducting film with $T_{c,\ onset}$ of 65K was prepared by annealing a film accumulating four layers of Bi_2O_3, SrF_2, CaF_2, and CuO at 850 C for 30min in air.

4-3. Deposition of Bi, Sr, Ca, and Cu Oxide Films by rf Glow Discharge Generated at Relatively High Pressure

4-3-1. Experimental

Figure 4-13 represents the setup of the apparatus used in the present study. The condenser type electrodes were specially designed to maintain the glow discharge at pressures as high as 1atm.[23)] The cathode electrode (30mmϕ) is composed of tungsten needles with a diameter of 0.2mm and the anode is covered with a quartz plate of 0.2mm thick. The substrate MgO(100) was heated at

400 °C. A mixture of plasma excited O_2 and Ar gases was introduced above the substrate to be mixed with the source materials carried on helium flow. Helium was indispensable for sustaining the glow discharge at pressures higher than 10Torr. Rf plasma in a high oxygen partial pressure was expected to facilitate the preparation of oxide films efficiently. Source materials employed were $Bi(C_6H_5)_3$, $Sr(DPM)_2$, $Ca(DPM)_2$, and $Cu(DPM)_2$, where DPM represents $(CH_3)_3CCOCHCOC(CH_3)_3$, supplied from Tri-chemical Co., Ltd. They were heated separately in oil baths and carried into the reaction chamber by helium. The evaporation temperature were determined by TG measurement under Ar 100Torr atmosphere using a Sinku-Riko TGD-7000RH model.(Fig. 4-14) To prevent the source materials from condensation, the gas lines were heated to 250 °C. The film thickness was determined by the stylus method using a Taylor-Hobson Talystep. The crystal structure and elemental composition were analyzed by X-ray diffraction (XRD: MAC Science MXP^3) and X-ray photoelectron spectroscopy(XPS: JEOL: JPS-80), respectively.

4-3-2. Results and Discussion

4-3-2-1. Film Preparation and Deposition Rate

Table 4-1 lists representative film preparation conditions. The relationship between the film thickness and reaction time was measured to confirm the proportional film growth. Figure 4-15 shows the results. In the cases of film deposition from $Bi(C_6H_5)_3$, $Sr(DPM)_2$, $Ca(DPM)_2$, and $Cu(DPM)_2$, fairly good linear relationships were observed at the film deposition rates of 1.30, 1.67, 1.25, and 1.50A/s, respectively. For $Cu(HFA)_2$, the linearity was not so good due probably to poor purity of the

source. Since the thickness of each oxide layers in Bi-Sr-Ca-Cu-O superconductor is 2~3A,[24] the thickness of each oxide film must be controlled at that order for layer-by-layer deposition. The deposition rates we obtained (1.25~1.67A/s) appear to be little too high for the purpose of such layer-by-layer deposition.

4-3-2-2. Crystal Structure and Composition of the Film

Figure 4-16 shows the X-ray diffraction pattern of the film prepared from $Cu(HFA)_2$ at a substrate temperature of 350 °C. The oxygen partial pressure in the reaction chamber was 0.45Torr. Peaks of CuO were detected. The contamination of fluorine and carbon from the ligand of $Cu(HFA)_2$ was not detected by XPS analysis. X-ray diffraction patterns of the films prepared from $Bi(C_6H_5)_3$, $Sr(DPM)_2$, $Ca(DPM)_2$, and $Cu(DPM)_2$ are shown in Fig. 4-17. The film as-deposited at a substrate temperature of 400°C from $Bi(C_6H_5)_3$ shows crystal structure of Bi_2O_3. Amorphous films were obtained from $Sr(DPM)_2$, $Ca(DPM)_2$, and $Cu(DPM)_2$ sources under the plasma CVD conditions listed in Table 4-1. Annealing the deposited amorphous films at 400°C in air turned them to crystals of $SrCO_3$, $CaCO_3$, and CuO, respectively.

The reason why crystalline films were not deposited from $Sr(DPM)_2$, $Ca(DPM)_2$, and $Cu(DPM)_2$ under the conditions of Table 4-1 should include (1) too low substrate temperature and (2) shortage of oxygen supply at the growing site. The former possibility is less probable, because the crystallization occurred by the subsequent annealing of the amorphous films at 400 °C in air. Synthetic reactions of Bi_2O_3 and MO(M=Sr, Ca, Cu) are represented as follows.

$$Bi(C_6H_5)_3+45/2O_2 \rightarrow Bi_2O_3+18CO_2+15/2H_2O$$

$$M(DPM)_2+32O_2 \rightarrow MO+22CO_2+19H_2O$$

For the completion of oxidation reaction, the amount of oxygen should exceed 22.5 and 32 molar equivalents to the source materials, respectively. Under the reaction conditions listed in Table 4-1 for $Ca(DPM)_2$, the molar ratio of $O_2/Ca(DPM)_2$ in the steady state is calculated to be 180. More than 17% of oxygen in feed must be consumed for the completion of oxidation reaction. This suggests that the latter possibility is a main reason why an oxide crystal structure was not detected in the as-deposited films. Figure 4-18 shows XRD patterns of as-deposited films prepared from $Ca(DPM)_2$ at reaction pressures of 3Torr and 10Torr. The crystal structure of the film prepared at a pressure of 3Torr was still amorphous, whereas the peaks identified to $CaCO_3$ were clearly observed in the film prepared at an elevated pressure of 10Torr. Thus, the author has verified that rf glow discharge under oxygen partial pressures higher than the conventional plasma CVD is a promising method for depositing artificially designed ceramic crystal films at a low temperature.

4-3-2-3. Preparation of a Superconducting Film

Four films were deposited successively under the conditions of Runs 1, 2, 3, and 4 in Table 4-1 from $Bi(C_6H_5)_3$, $Sr(DPM)_2$, $Ca(DPM)_2$, and $Cu(DPM)_2$. Each layer was designed to have thickness of 1000A. The stacked film was annealed at 850 °C in air for 30min. Low temperature resistivity was measured by conventional four probe method. $T_{c,\ onset}$ was observed at 80K as Fig. 4-19 shows. Weak peaks assigned to $Bi_2Sr_2CaCu_2O_x$ appeared in XRD pattern of the film. It is expected that stacking a number of

more thinner layers will bear superconducting film with higher quality.

4-3-3. Conclusion

Crystalline Bi_2O_3, $SrCO_3$, $CaCO_3$, and CuO films were prepared by rf plasma assisted CVD at a temperature of 400 °C. Increase of oxygen partial pressure was effective to prepare as-grown crystalline films. The accumulation of these four layers of about 1000A thick each at 400°C and subsequent annealing at 850°C gave a film indicating a superconductivity at 80K.

4-4. General Conclusion

Application of microwave or rf plasma to CVD of oxide films relating to high-T_c superconductor was effective to decrease substrate temperature. By accumulating each oxide and subsequent annealing, superconducting oxide films were successfully prepared.

References

1) T. Terashima, K. Iijima, K. Yamamoto, Y. Bando and H. Mazaki: Jpn. J. Appl. Phys., 27 (1988) L91.

2) S. Witanachchi, H. S. Kwok, S. W. Wang and D. T. Shaw: Appl. Phys. Lett., 53 (1988) 234.

3) S. Nagata, M. Kawasaki and H. Koinuma: Jpn. J. Appl. Phys., 27 (1988) L870.

4) D. D. Berkley, B. R. Johnson, N. Anand, K. M. Beauchamp, L. E. Conroy, A. M. Goldman, J. Maps, K. Mauersberger, M. L. Mecartney, J. Morton, M. Tuominen and Y. J. Zhang: Appl. Phys. Lett., 53 (1988) 1973.

5) T. Kawai, M. Kanai, H. Tabata and S. Kawai: the Proc. of the

Conf. on the Thin Film Superconductors, Nov. 14-18 (1988) Colorado Springs, Colorado

6) S. Watanabe, M. Kawai and T. Hanada: Jpn. J. Appl. Phys., 29 (1990) L1111.

7) H. Tabata, T. Kawai, M. Kanai, O. Murata and S. Kawai: Jpn. J. Appl. Phys., 28 (1989) L823.

8) H. Koinuma, H. Nagata, A. Takano, M. Kawasaki and M. Yoshimoto: Jpn. J. Appl. Phys., 27 (1988) L1887.

9) H. Adachi, S. Kohiki, K. Setsune, T. Mitsuyu and K. Wasa: Jpn. J. Appl. Phys., 27 (1988) L1883.

10) K. Nakamura, J. Sato, M. Kaise and K. Ogawa: Jpn. J. Appl. Phys., 28 (1989) L437.

11) D. G. Schlom, A. F. Marshall, J. T. Sizemore, Z. J. Chen, J. N. Eckstein, I. Bozovic, K. E. von Dessonneck, J. S. Harris, Jr. and J. C. Bravman: to be published in J. Cryst. Growth.

12) H. Koinuma and M. Yoshimoto: Function and Materials (Kino Zairyo), 10 No. 12 (1990) 5. (in Japanese): P. E. Norris and G. W. Orlando: Superconducor Industry, Spring 3 (1990) 14

13) K. Watanabe, H. Yamane, H. Kurosawa, T. Hirai, N. Kobayashi, H. Iwasaki, K. Noto and Y. Muto: Appl. Phys. Lett., 54 (1989) 575.

14) A. D. Berry, D. K. Gaskill, R. T. Holm, E. J. Cukauskas, R. Kaplan and R. J. Henry: Appl. Phys. Lett., 52 (1988) 1743.

15) K. Kanehori, N. Sugii and K. Miyauchi: MRS Fall Meeting (1988) M7. 172.

16) J. Zhao, D. W. Noh, C. Chern, Y. Q. Li, P. Norris, B. Gallios and B. Kear: Appl. Phys. Lett., 56 (1990) 2342.

17) K. Kobayashi, S. Ichikawa and G. Okada: Chem. Lett., 1989

(1989) 1415.

18) T. Hashimoto, T. Kosaka, Y. Yoshida and H. Koinuma: Mol. Cryst. Liq. Cryst., 184 (1990) 207.

19) T. Hashimoto, K. Fukuda, M. Kogoma, S. Okazaki, M. Yoshimoto and H. Koinuma: Mol. Cryst. Liq. Cryst. 184 (1990) 201.

20) K. J. Eisentraut and R. E. Sievers: J. Inog. Nucl. Chem., 29 (1967) 1931.: J. E. Schwarberg, R. E. Sievers and R. W. Moshier: Annal. Chem. 42 (1970) 1828.: R. Belcher, K. Belessel, T. Cardwell, M. Pravica, W. I. Stephan and P. C. Uden: J. Inog. Nucl. Chem., 35 (1973) 1127.

21) M. Okada, M. Amamiya, S. Takai and T. Araki: Extended Abstracts of the 49th Autumn Meeting, 1988, The Japan Society of Applied Physics, 487, 7a-V-2. (in Japanese).

22) T. Asano, H. Ishiwara and N. Kaifu: Jpn. J. Appl. Phys., 22 (1983) 1474.

23) S. Kanazawa, S. Kogoma, T. Moriwaki and S. Okazaki: the Proc. of the 8th Int'l Symp. on Plasma Chem., 3 (1987) 1839.

24) R. M. Hazen, L. W. Finger, R. J. Angel, C. T. Prewitt, N. L. Ross, C. C. Hadidiacos, P. J. Heaney, D. R. Veblen, Z. Z. Sheng, A. EL. Ali and A. M. Herman: Phys. Rev. Lett., 60 (1988) 1657.

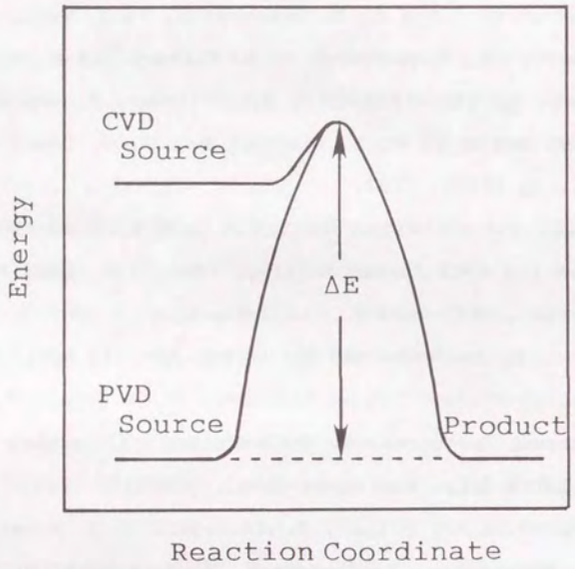

Fig. 4-1. Schematic energy diagram of PVD and CVD.

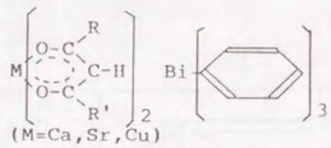

Abbreviation	Name	R	R'
DPM	dipivaloylmethane	$C(CH_3)_3$	$C(CH_3)_3$
HFA	hexafluoroacetylacetonato	CF_3	CF_3
PPM	pentafluoropivaloylmethane	C_2F_5	$C(CH_3)_3$

Fig. 4-2. Structures of CVD source materials used in this study.

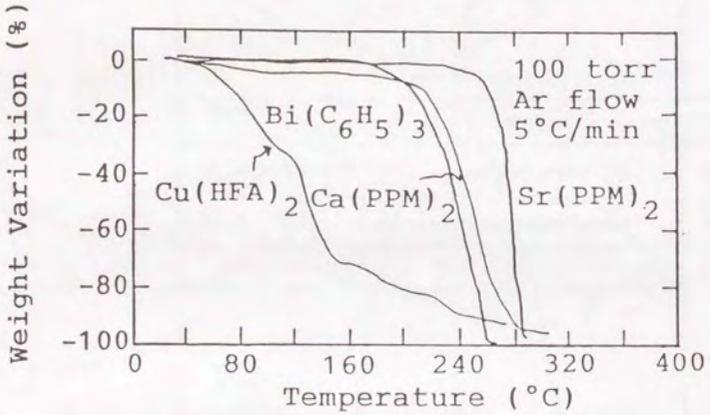

Fig. 4-3. TG curves of the source materials used in this study.

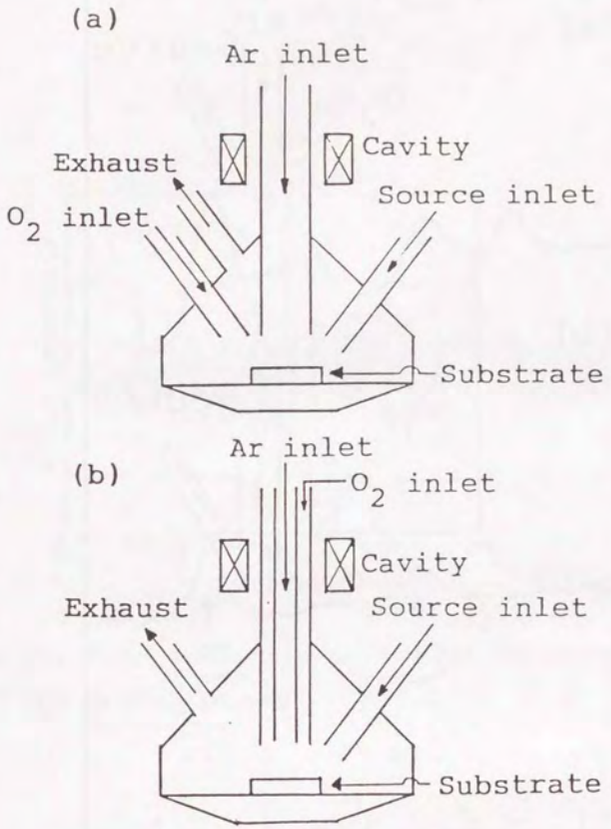

Fig. 4-4 Schematic diagram of 2.45GHz microwave CVD apparatus. Oxygen and Ar were supplied by separate tubings (a) or double quartz tubing (b).

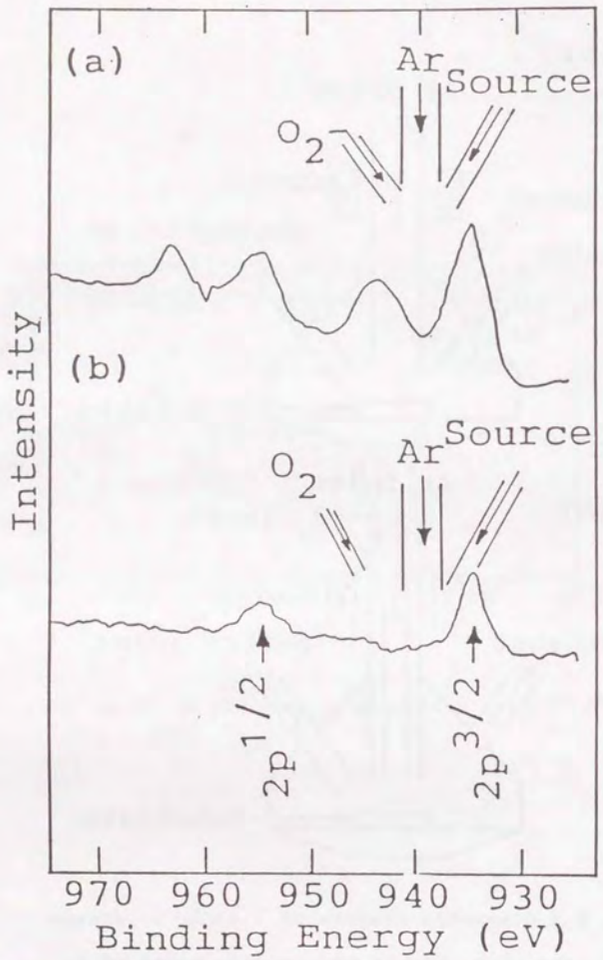

Fig. 4-5. XPS spectra of Cu 2p peaks of the films prepared from $Cu(HFA)_2$ at a substrate temperature of 600°C. The distance between the oxygen and Ar inlets were (a)0.5cm (b)3cm.

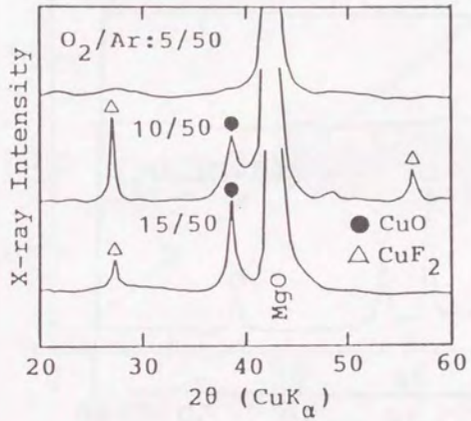

Fig. 4-6. X-ray diffraction patterns of the films prepared at 400°C from $Cu(HFA)_2$ at various O_2/Ar ratio.

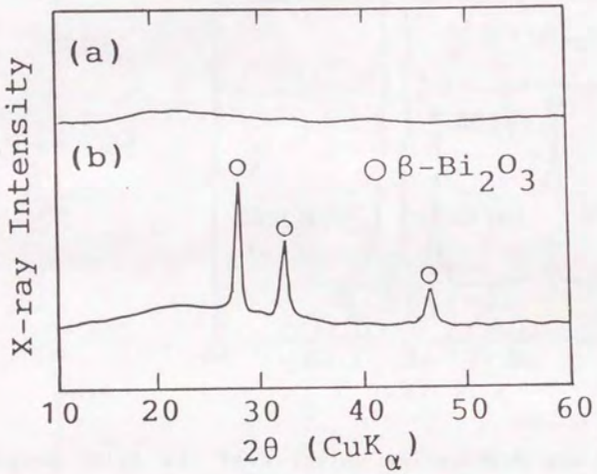

Fig. 4-7. X-ray diffraction patterns of the film prepared from $Bi(C_6H_5)_3$ at microwave power of (a)60W and (b)90W. The substrate temperature was 200°C.

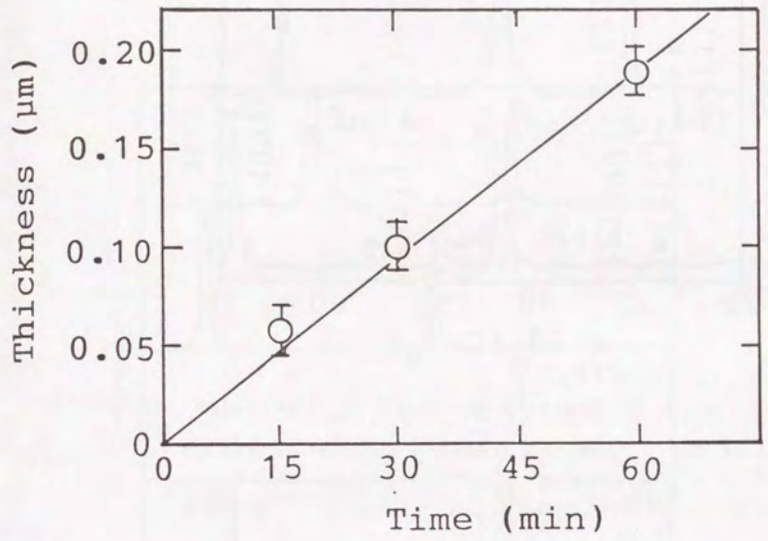

Fig. 4-8. Dependence of Bi_2O_3 film thickness on reaction time. Deposition rate was constant at 0.56A/s.

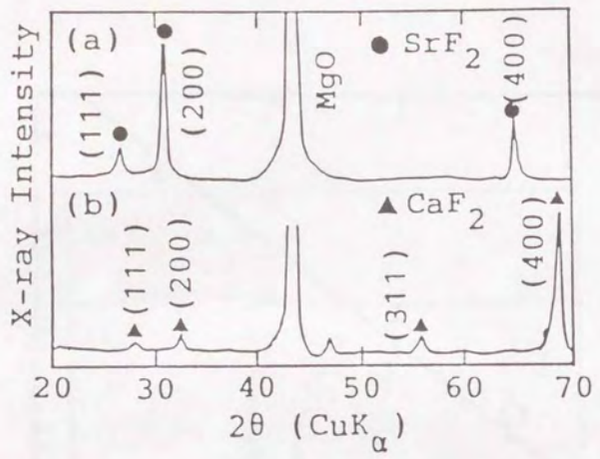

Fig. 4-9. X-ray diffraction patterns of the films on MgO(100) prepared at 400 °C from (a) $Sr(PPM)_2$ and (b) $Ca(PPM)_2$.

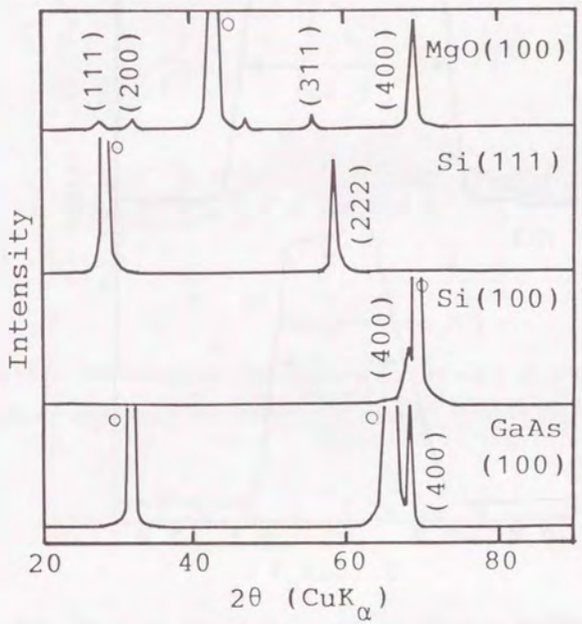

Fig. 4-10. X-ray diffraction patterns of the CaF_2 films prepared from $Ca(PPM)_2$ on various substrates. ○ peaks indicates diffraction from substrates.

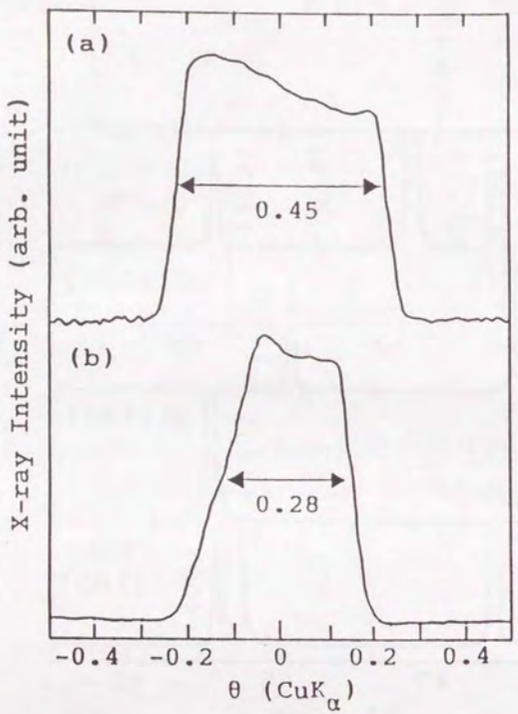

Fig. 4-11. Rocking curves of the CaF_2(222) peak of the films prepared from $Ca(PPM)_2$ on Si(111). Film deposition rates were (a)3.6Å/s and (b)1.3Å/s.

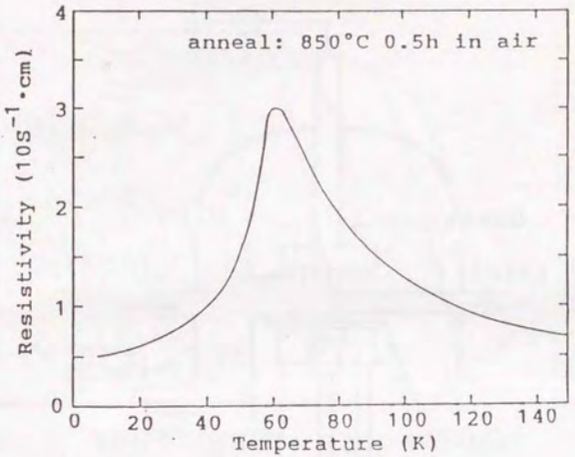

Fig. 4-12. Temperature dependence of resistivity of the layered film after annealed at 850°C for 30min.

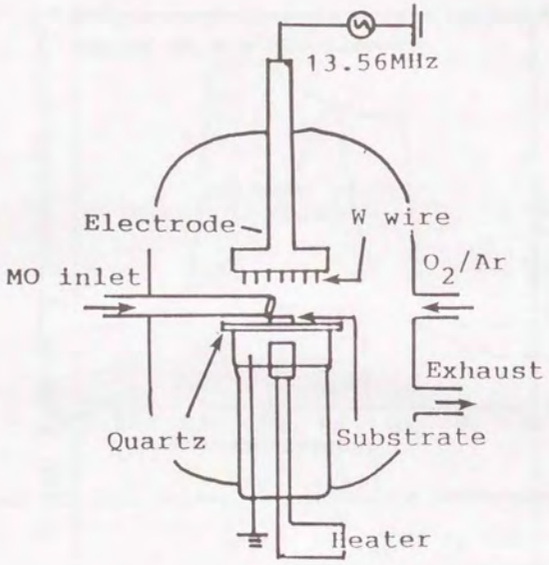

Fig. 4-13. Schematic representation of plasma CVD chamber which enables rf glow discharge at relatively high pressures.

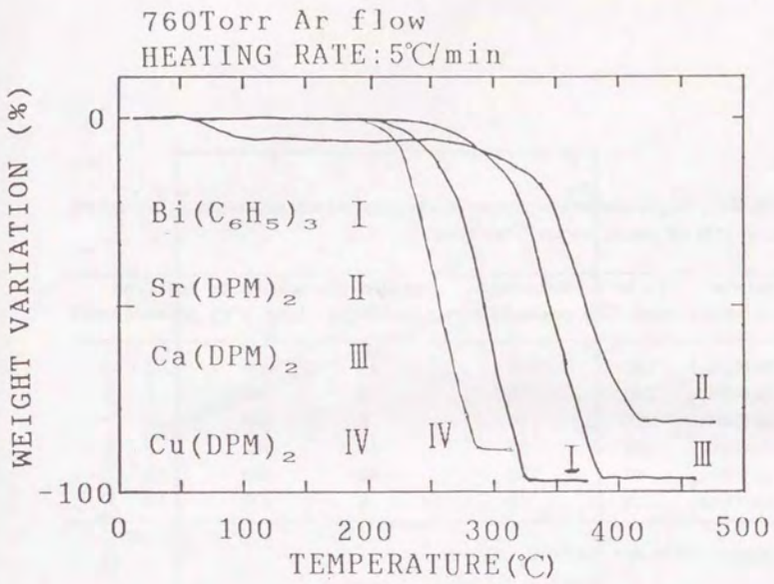

Fig. 4-14. TG curves of the sources employed for the film preparation by rf plasma CVD.

Table 4-1. Representative preparation conditions of oxide films by rf plasma CVD of metal organic sources.

	Source material	Oil bath temp.(°C)	Evaporator press.(Torr)	Carrier gas flow(sccm)	Substrate temp.(°C)	Reaction press.(Torr)
#1	$Bi(C_6H_5)_3$	130	100	40	400	3
#2	$Sr(DPM)_2$	240	10	6	400	3
#3	$Ca(DPM)_2$	220	10	6	400	3
#4	$Cu(DPM)_2$	140	100	40	400	3
#5	$Cu(HFA)_2$	80	100	40	350	10
#6	$Ca(DPM)_2$	220	10	6	400	10

rf power: 100W Ar: 2sccm O_2: 2sccm

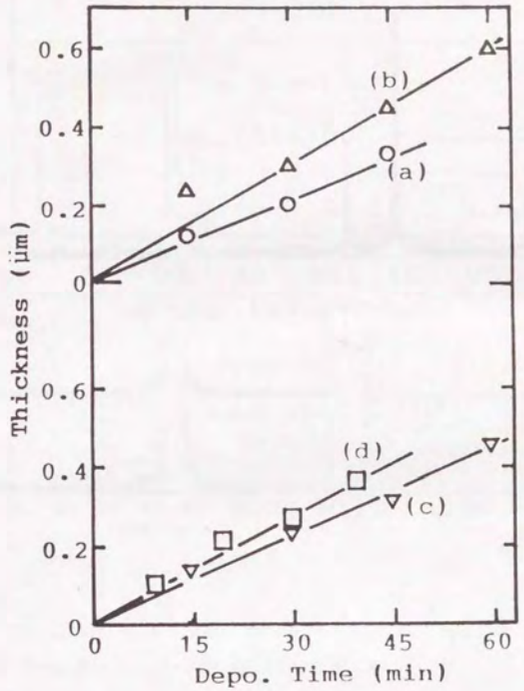

Fig. 4-15. Time dependence of film thickness prepared from (a)$Bi(C_6H_5)_3$, (b)$Sr(DPM)_2$, (c) $Ca(DPM)_2$, and (d) $Cu(DPM)_2$.

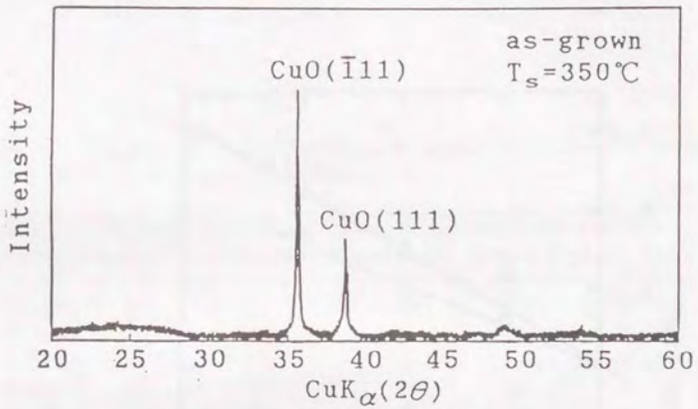

Fig. 4-16. X-ray diffraction pattern of the film prepared from $Cu(HFA)_2$.

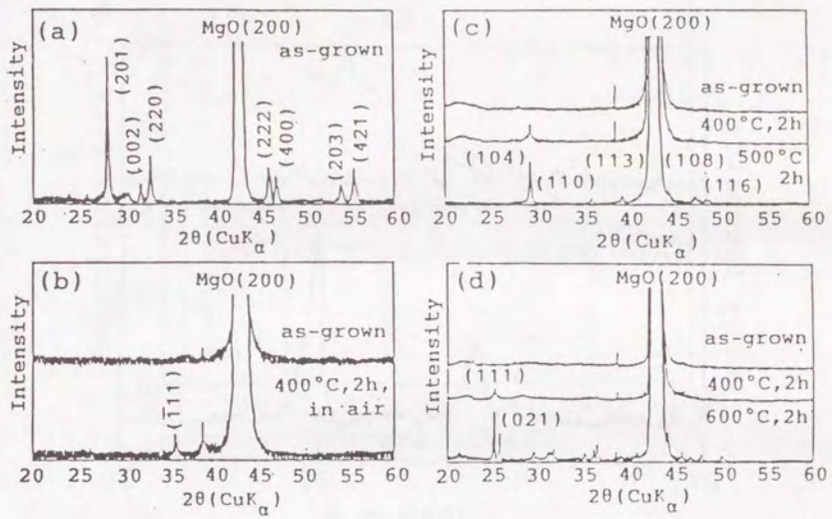

Fig. 4-17. X-ray diffraction patterns of the as-deposited films prepared from (a) $Bi(C_6H_5)_3$, (b) $Cu(DPM)_2$, (c) $Ca(DPM)_2$ and (d) $Sr(DPM)_2$. As for deposition conditions, see Table 4-1.

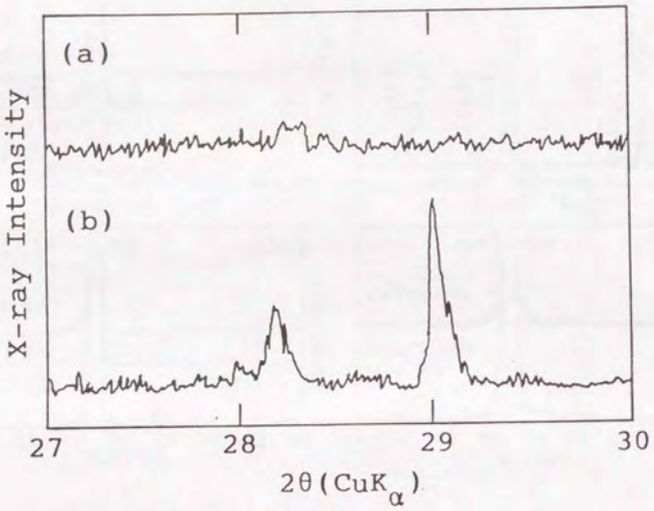

Fig. 4-18. X-ray diffraction patterns of the films prepared from $Ca(DPM)_2$ at reaction pressures of (a) 3Torr and (b) 10Torr.

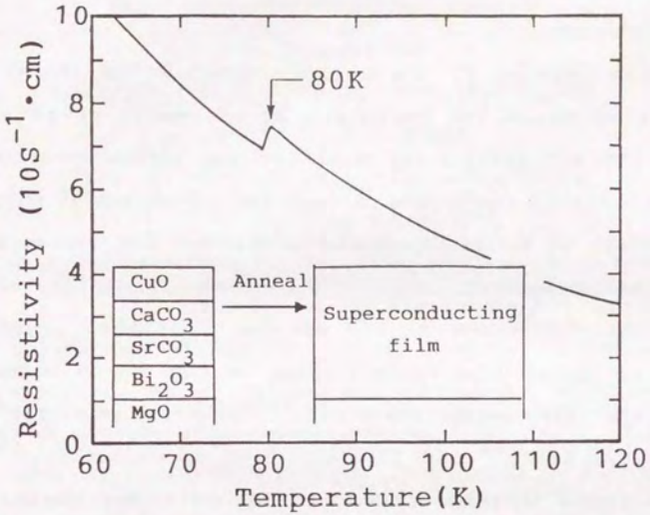

Fig. 4-19. Temperature dependence of resistivity of the layered film after annealed at 850°C for 30min.

Chapter 5

Purification and UV-VIS Light Absorption Property of Source Materials for CVD of High-T_c Superconducting Films

5-1. Introduction

In the chapter 4, the author reported low temperature synthesis of oxide and carbonate by microwave or rf plasma assisted CVD and preliminary data for the accumulation of the films. In order to accumulate oxide films, thickness of which are atomic order, it is indispensable to control the source supply more precisely. However, relatively poor reproducibility of data is frequently observed in CVD of high-T_c films, presumably originating partly from contamination in the source materials. Although the vaporization pressures,[1-3] thermogravimetric[4] and mass spectra data,[5] and IR absorption spectroscopy,[6] were reported using sources whose purities were not checked, no systematic and quantitative studies have been made on the purification process or characterization of the CVD source materials. In this chapter, the author reports elucidation of the purification process and evaluation of the purity of source materials. The UV-VIS (ultraviolet and visible light absorption) spectral data of the sources were also collected to estimate the possibility of photo-CVD which could be another possible method of low-temperature film deposition.[7]

5-2. Experimental

$Bi(C_6H_5)_3$, $Sr(DPM)_2$, $Ca(DPM)_2$ and $Cu(DPM)_2$ (DPM: dipyvaloylmethane $(CH_3)_3CCOCH_2COC(CH_3)_3$: IUPAC name is 2,2,6,6-tetramethyl-3,5-heptanedione) complexes were prepared by the chemical reactions given below, supplied in purified form from

Tri-chemical Co., Ltd., Nihonsanso Co., Ltd. and Nihon Kagaku Sangyo Co., Ltd.

$$BiCl_3+3C_6H_5MgBr \rightarrow Bi(C_6H_5)_3+3MgClBr$$

in diethylether

$$Sr+2(CH_3)_3CCOCH_2COC(CH_3)_3 \rightarrow Sr(C_{11}H_{19}O_2)_2+H_2$$

in n-hexane

$$Ca+2(CH_3)_3CCOCH_2COC(CH_3)_3 \rightarrow Ca(C_{11}H_{19}O_2)_2+H_2$$

in n-hexane

$$Cu(NO_3)_2\cdot 3H_2O+2(CH_3)_3CCOCH_2COC(CH_3)_3+2NH_4OH \rightarrow Cu(C_{11}H_{19}O_2)_2+2NH_4NO_3+5H_2O$$

in n-hexane

Each supplied complex was further purified by sublimation in a glass apparatus as illustrated in Fig.5-1. An evaporation pressure of 20mTorr and temperatures of 95 °C, 140°C, 200° C, and 240 °C were employed for $Bi(C_6H_5)_3$, $Cu(DPM)_2$, $Ca(DPM)_2$ and $Sr(DPM)_2$, respectively. The TG-DTA (thermogravimetry-differential thermal analysis) was measured in 1atm Ar flow at a heating rate of 10 °C/min using a Seiko TG/DTA-320. The IR (infrared absorption) and ^{1}H-NMR (nuclear magnetic resonance) spectra were recorded on each specimen before and after the purification. The IR spectra were measured using a Shimadzu IR-470 on disc samples made by pressing a mixture of the complex and KBr powders. ^{1}H-NMR spectroscopy was performed using a JEOL NM3974 spectrometer for samples dissolved in $CDCl_3$ containing about 3% tetramethylsilane as a reference. The UV-VIS spectra were measured by a Hitachi 200-20 spectrometer on hexane solutions of 1, 2, 5, 7, 10×10^{-5}mol/l in the wavelength range between 190nm and 900nm.

5-3. Results and Discussion

5-3-1 $Bi(C_6H_5)_3$ and $Cu(DPM)_2$

Table 5-1 summarizes the sublimation conditions and C and H contents for the complexes before and after the sublimation. The C and H contents were kept constant within 0.3% of the authentic values. The colors, TG-DTA curves(Figs. 5-2 and 5-3; At 80°C, endothermic peak corresponding to melting point was observed in DTA curves of $Bi(C_6H_5)_3$. Weight decrease start from 135°C and 150°C and all sample was perfectly sublimated at 283°C and 266°C for $Bi(C_6H_5)_3$ and $Cu(DPM)_2$, respectively.), IR and NMR spectra were also unchanged by the sublimation and no significant amounts of impurities were detected by these analyses.

5-3-2 $Ca(DPM)_2$

$Ca(DPM)_2$ was sublimated at 200°C. Although no appreciable change was observed in C and H contents (see Table 5-1) as well as in the sample color (white), slight variations were observed in the TG curves (Fig. 5-4) and ^{1}H-NMR spectra (Fig. 5-5) by the sublimation. The peaks at 45°C and 64°C in the differential TG curve, both corresponding to weight decrease, disappeared after sublimation. The main ^{1}H-NMR peaks at 1.06ppm and 5.67ppm can be assigned, respectively, to the tertiary buthyl protons and the proton bonded to the carbon between the two carbonyl groups in DPM of $Ca(DPM)_2$. In the spectrum of pre sublimation, minor additional ^{1}H-NMR peaks were observed at 1.02ppm and 5.58ppm, which can be assigned to the tertiary buthyl and methylene protons in the dipyvaloylmethane ligand which is not coordinated to calcium, respectively. From the relative area ratio of the 1.06ppm peak to the 1.02ppm peak, the purity of as-supplied and sublimated

$Ca(DPM)_2$ were evaluated to be 91% and 100%, respectively. Thus, free dipyvaloylmethane was completely removed by the sublimation.

5-3-3 $Sr(DPM)_2$

Pale yellow as-supplied compound was evaporated by heating in a pressure of 20mTorr at 150°C and subsequently at 240°C to deposit yellow grains and white powders, respectively, on the surface of a dry ice-cooled inner flask. The yellow grains can be identified as free dipyvaloylmethane ligand, since their elemental analysis given in Table 5-1 agreed well with the value calculated for $C_{11}H_{19}O_2$. Figure 5-6 shows the ^{1}H-NMR spectra of three specimens, one before the sublimation and the others of the yellow and white sublimates. The ^{1}H-NMR spectra of yellow grains reinforce the assignment to dipyvaloylmethane. Three peaks were observed in ^{1}H-NMR spectra of as-supplied $Sr(DPM)_2$ at 1.03ppm, 1.20ppm, and 1.35ppm that could be assigned, respectively, to the tertiary buthyl protons in $Sr(DPM)_2$, to those in free dipyvaloylmethane, and to an unknown impurity. The peak at 1.03ppm was observed exclusively in the ^{1}H-NMR spectra of the white sublimate, indicating that the purity of $Sr(DPM)_2$ was substantially improved by the sublimation. Recrystallization prior to the sublimation was examined for further purification of $Sr(DPM)_2$. Although recrystallization of $Sr(DPM)_2$ from ethanol solution was already reported,[8] its effect was not discussed. The as-supplied sample of 5.0g was solved in 11g ethanol, which had been distilled in the presence of CaO, at 40°C and cooled at -30°C for 3 days. The precipitated rectangular crystals were dried in vacuo at 180°C for 6h to give white powders (3.6g). They could be sublimated at a temperature as low as 195°C, a

significant decrease from the 240 °C required for the as-supplied reagent. The C and H contents of the sublimate were remarkably improved, as shown in Table 5-1. Figure 5-7 shows ^{1}H-NMR spectra of the sublimated sample. From the relative intensity of very small peaks still remaining at 1.20ppm and 1.35ppm to the main peak at 1.03ppm, the purity of $Sr(DPM)_2$ is estimated to be improved from 85% to 95%. The TG curves of the $Sr(DPM)_2$ measured before and after the recrystallization-sublimation are shown in Fig. 5-8. The weight decrease exceeds 95% in the refined sample. The purity should be further improved by repeating the sequential purification procedure.

5-3-4 Light Absorption Property (UV-VIS Spectra) of Source Materials

Figure 5-9 shows UV-VIS spectra of hexane solutions ((a)~(d)7×10^{-5}mol/l,(e) 2×10^{-5}mol/l) of the $Bi(C_6H_5)_3$, $Sr(DPM)_2$, $Ca(DPM)_2$, and $Cu(DPM)_2$ purified by the methods described above. The pattern of UV absorption spectrum showed good correspondence to the pattern reported by Fackler et. al.[9] For all of the sources, strong light absorption was observed in the range from 190nm to 320nm but not in the range from 320nm to 900nm. Except for $Bi(C_6H_5)_3$, the light absorption obeyed Lambert-Beer's law as Figs. 5-10, 5-11, and 5-12 show, making it possible to evaluate the molar absorption coefficients. The UV-VIS absorption pattern of $Bi(C_6H_5)_3$ was strongly dependent on the solution concentration. As Figure 5-13 depicts, the maximum absorption of $Bi(C_6H_5)_3$ shifted to the longer wavelength at the higher concentration, clearly indicating the aggregation of $Bi(C_6H_5)_3$ in

this concentration range.

Table 5-2 lists the molar absorption coefficients of $Bi(C_6H_5)_3$, $Sr(DPM)_2$, $Ca(DPM)_2$, and $Cu(DPM)_2$ at several wavelengths frequently used in photo-CVD of various kinds of thin films. At 249nm (KrF excimer laser) and 254nm (low-pressure mercury lamp), the absorption coefficients are in the range of 10^3~10^4 l/mol·cm. Although the light absorption behaviors may be slightly different from those in hexane solution, the examined concentration range of 10^{-5}~10^{-4}mol/l corresponds to the pressure range of photo-CVD (0.2-2.0Torr). Thus, these source materials have a high potential as good sources for photo-CVD using a low-pressure mercury lamp or a KrF excimer laser. Studies on photo-CVD of oxide films by oxidative decomposition of each and of mixed sources are reported in the next chapter.

5-4. Conclusion

Purification and spectral properties of source materials for CVD of high-T_c superconducting films have been investigated quantitatively. Based on elemental analysis, TG, IR spectroscopy, and ^{1}H-NMR spectroscopy, sublimation was verified to be satisfactory for the purification of $Bi(C_6H_5)_3$, $Ca(DPM)_2$, and $Cu(DPM)_2$(DPM: dipyvaloylmethane). $Sr(DPM)_2$ was not sufficiently purified by the sublimation alone, but recrystallization from an ethanol solution in advance improved the purity of the sublimate, as verified by a significant decrease in the sublimation temperature. The UV-VIS spectra revealed that $Bi(C_6H_5)_3$, $Sr(DPM)_2$, $Ca(DPM)_2$ and $Cu(DPM)_2$ had high absorption coefficients at wavelengths around 254nm, suggesting high possibilities of their photochemical decomposition by light irradiation from a low-pressure mercury lamp.

References

1) S. Yuhya, K. Kikuchi, M. Yoshida, K. Sugawara and Y. Shiohara: Mol. Cryst. Liq. Cryst., 184 (1990) 231.

2) T. Abe, R. Ogawa and Y. Kuniya: Extended Abstracts of the 49th Autumn Meeting of the Japan Society of Applied Physics, Toyama, (1988) 116. (in Japanese)

3) N. Seo, Y. Matsumiya and Y. Kuniya: Extended Abstracts of the 36th Spring Meeting of the Japan Society of Applied Physics, Chiba, (1989) 104.(in Japanese)

4) K. Shimohara, F. Munakata and M. Yamanaka: Jpn. J. Appl. Phys., 27 (1988) L1683.

5) H. Zama and S. Oda: Jpn. J. Appl. Phys., 29 (1990) L1072.

6) H. Harima, H. Ohnishi, K. Hanaoka, K. Tachibana, M. Kobayashi and S. Hoshinouchi: Jpn. J. Appl. Phys., 29 (1990) 1932.

7) H. Koinuma and M. Kawasaki: Oyo Buturi (Applied Physics), 56 (1987) 332.(in Japanese)

8) G. S. Hammond, D. C. Nonhebel and C. S. Wu: Inog. Chem., 2 (1963) 73.

9) J. P. Fackler, Jr., F. A. Cotton and D. W. Barnum: Inorg. Chem., 2 (1963) 97.

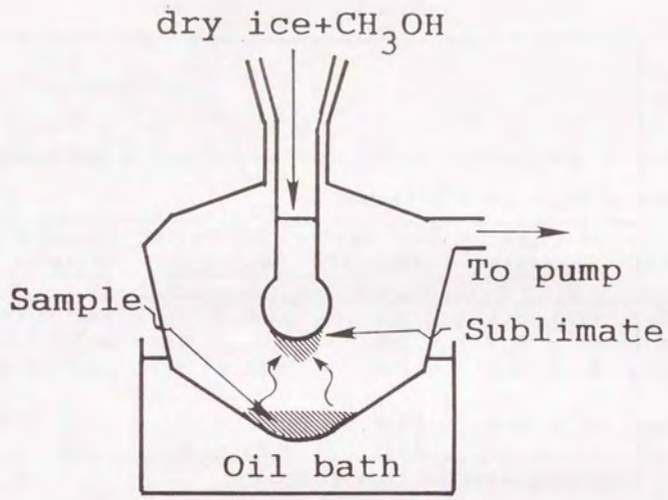

Fig. 5-1. Schematic diagram of sublimation apparatus.

Table 5-1. Sublimation conditions and C and H contents of as-supplied samples and sublimates.

Material	As-supplied sample(%)		Sublimation Temp.(°C)	Sublimated sample(%)		Calculated value(%)	
	C	H		C	H	C	H
$Bi(C_6H_5)_3$	49.3	3.6	95	49.2	3.5	49.1	3.4
$Cu(DPM)_2$	61.5	8.9	140	61.2	9.2	61.4	8.9
$Ca(DPM)_2$	64.7	9.6	200	64.8	9.7	64.9	9.4
$Sr(DPM)_2$	57.5	8.3	150	73.0	10.2	58.2	8.4
			240	52.4	8.0		
			195*	57.6	8.2		

*After recrystallization from ethanol

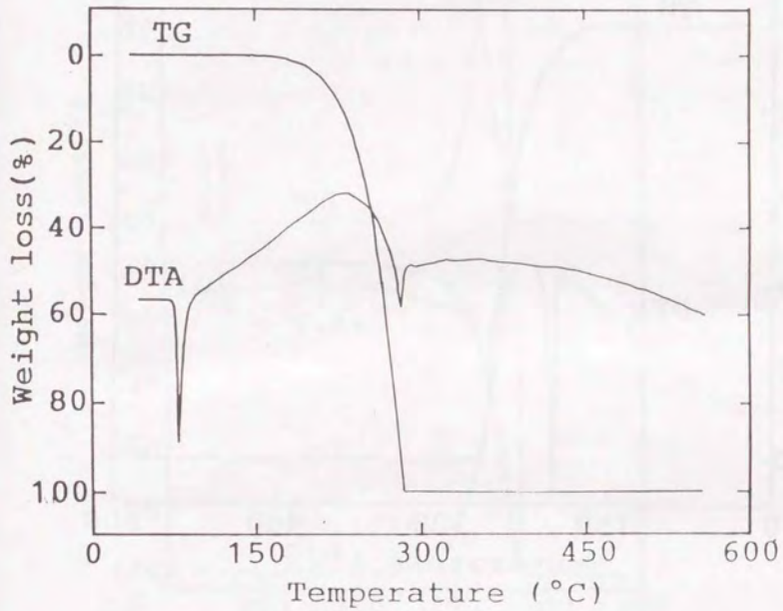

Fig. 5-2. TG-DTA curves of $Bi(C_6H_5)_3$ at Ar 1atm atmosphere. Heating rate was 10°C/min.

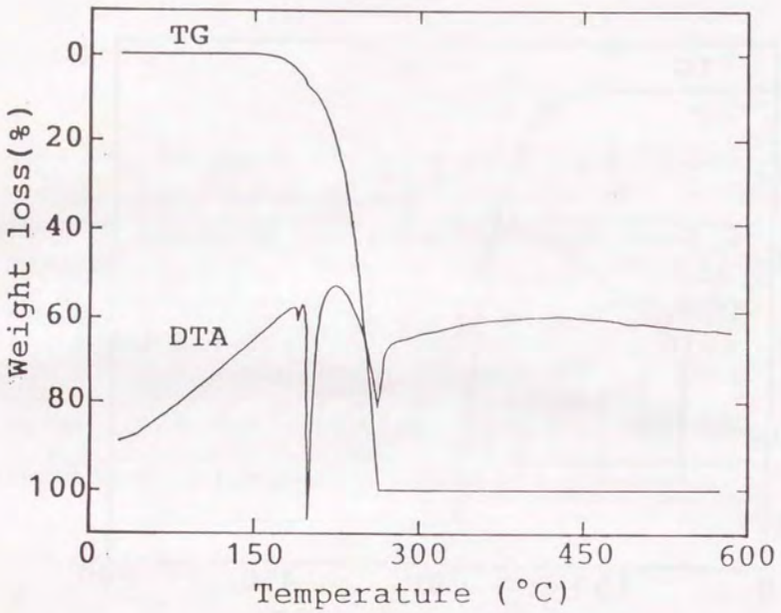

Fig. 5-3. TG-DTA curves of $Cu(DPM)_2$ at Ar 1atm atmosphere. Heating rate was 10°C/min.

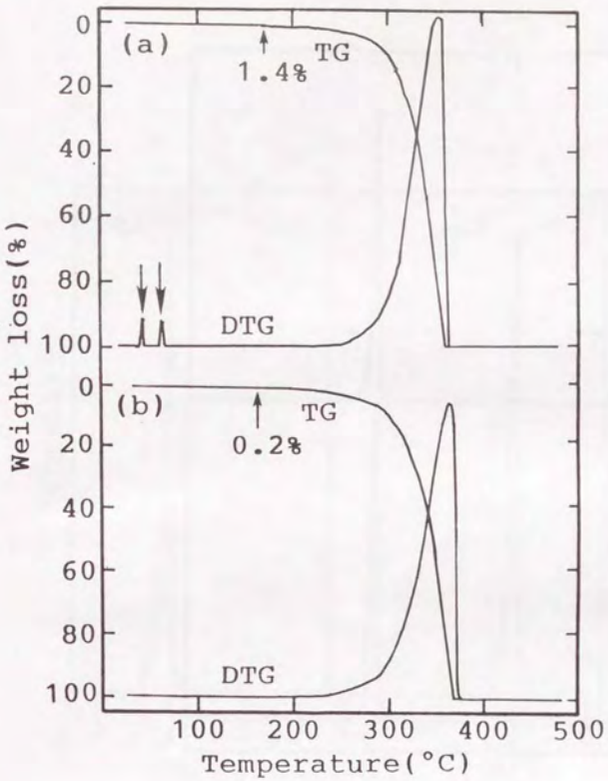

Fig. 5-4. TG and differential TG curves of (a) $Ca(DPM)_2$ before sublimation and of (b) sublimate under Ar 1atm atmosphere. Initial sample weight and heating and cooling rate were 15.0mg and 10 °C/min, respectively. The value in the figure is weight decrease at 64 °C. Differential TG peaks in (a) indicated with arrows were not observed in (b).

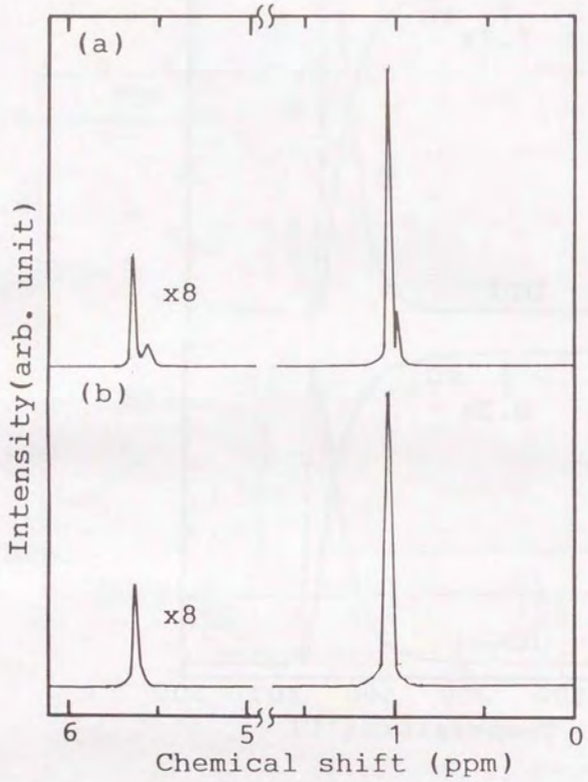

Fig. 5-5. ^{1}H-NMR spectra of (a)Ca(DPM)$_2$ before sublimation and of (b) sublimate at 200°C.

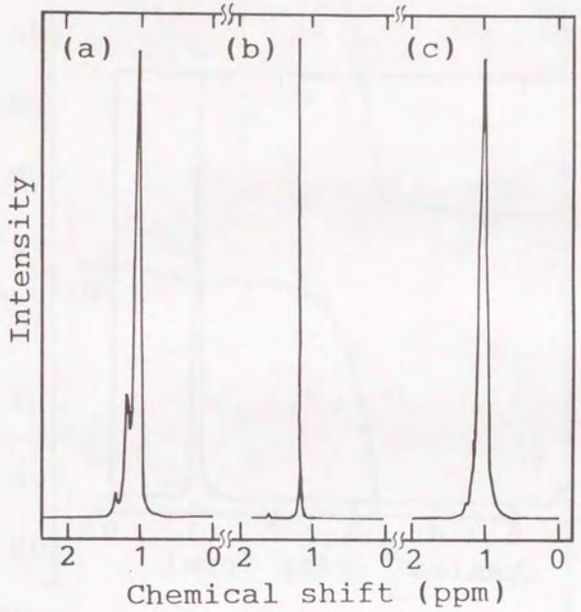

Fig. 5-6. ^{1}H-NMR spectra of (a) Sr(DPM)$_2$ before sublimation, of (b) yellow grains sublimated at 150°C, and of (c) white sublimate at 240°C.

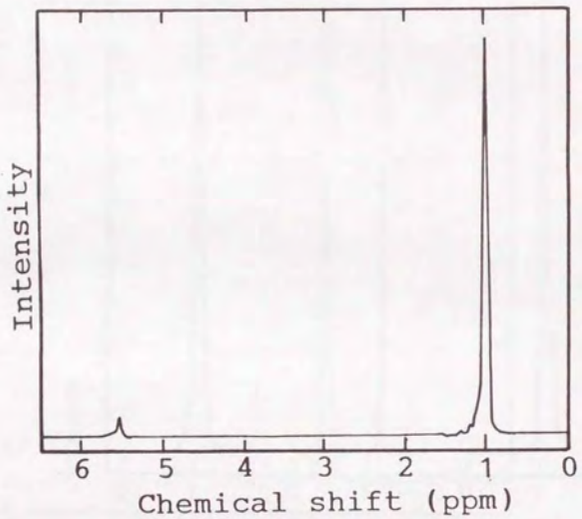

Fig. 5-7. ^{1}H-NMR spectrum of recrystallized and subsequently sublimated $Sr(DPM)_2$.

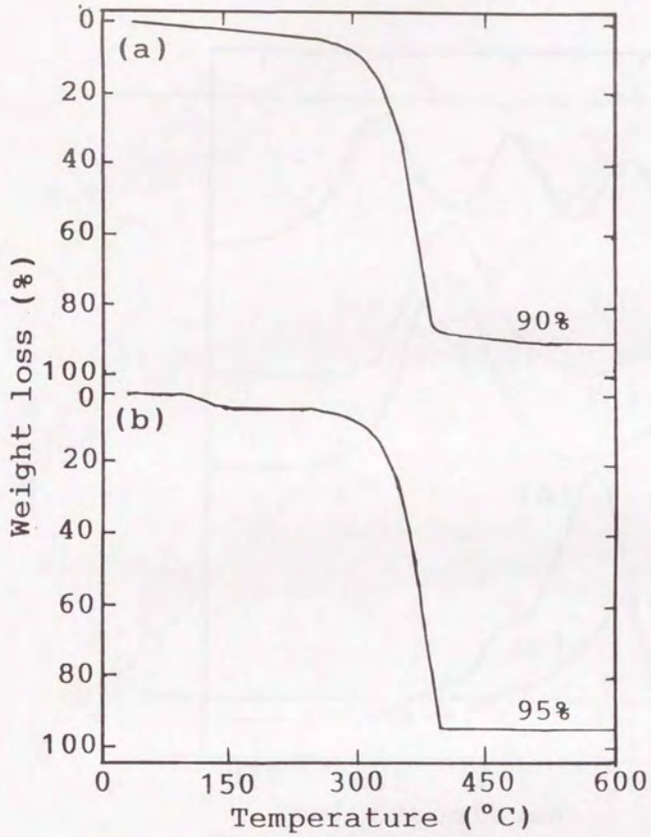

Fig. 5-8. TG curves of (a) as-supplied $Sr(DPM)_2$ and of (b) $Sr(DPM)_2$ after recrystallization and sublimation under Ar 1atm atmosphere. Initial sample weight and heating rate were 15.0mg and 10 ℃/min, respectively.

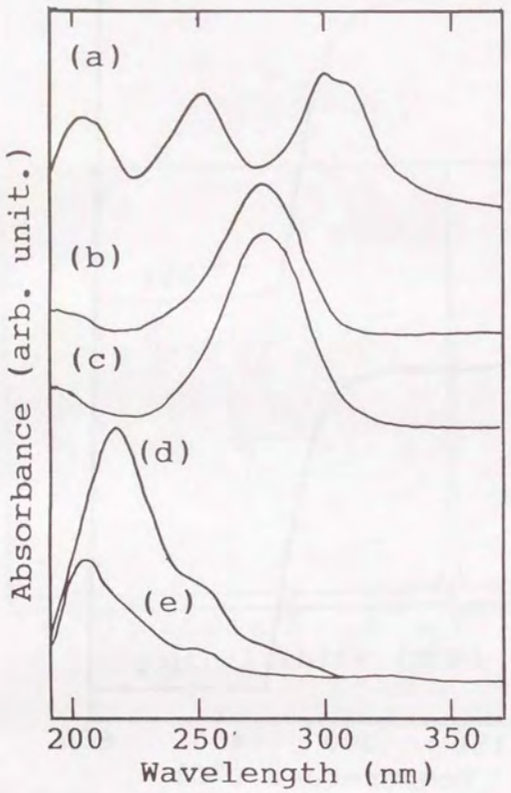

Fig. 5-9. UV-VIS spectra of 7×10^{-5} mol/l hexane solution of (a) $Cu(DPM)_2$, (b) $Ca(DPM)_2$, (c) $Sr(DPM)_2$ and (d) $Bi(C_6H_5)_3$. The UV-VIS spectrum of 2×10^{-5} mol/l of $Bi(C_6H_5)_3$ is also depicted in (e).

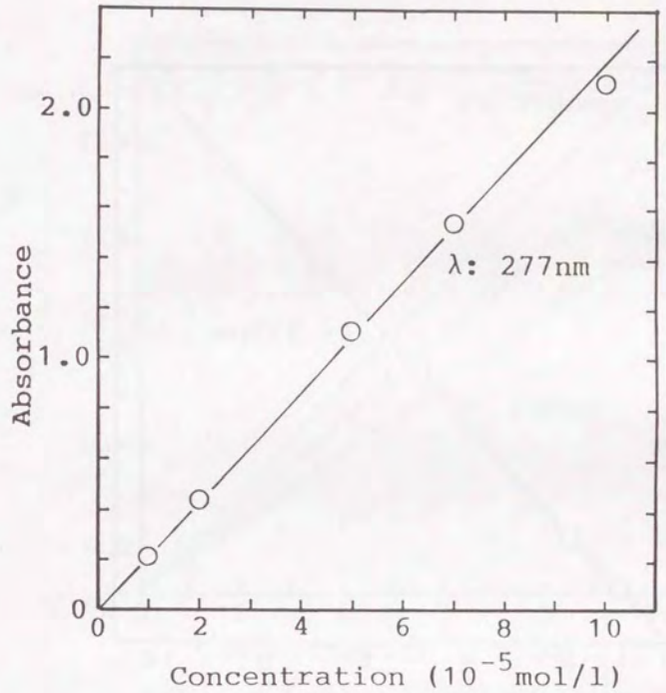

Fig. 5-10. The relationship between absorbance vs. concentration of hexane solution of $Sr(DPM)_2$.

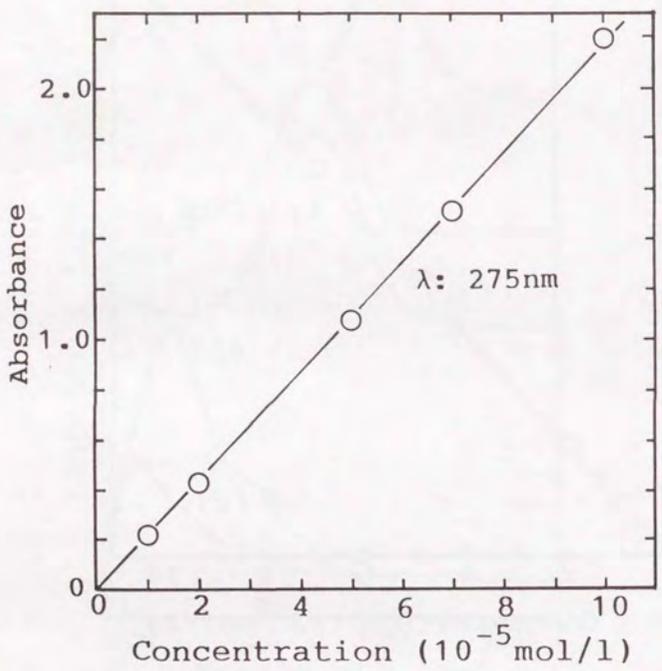

Fig. 5-11. The dependence of absorbance on concentration of $Ca(DPM)_2$ hexane solution.

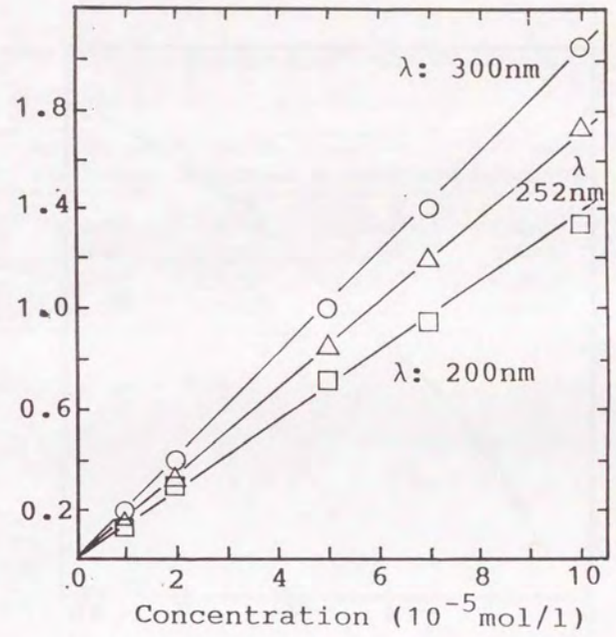

Fig. 5-12. Absorbance vs. concentration relationship of hexane solution of $Cu(DPM)_2$.

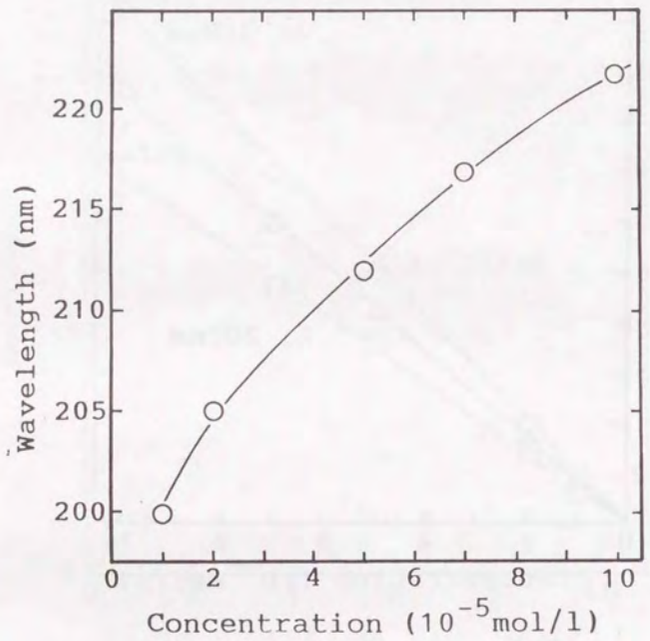

Fig. 5-13. The dependence of wavelength at maximum absorption on $Bi(C_6H_5)_3$ concentration. The solvent was hexane.

Table 5-2. Molar absorption coefficients of hexane solutions of source materials at various wavelength.

Material	ArF excimer laser(193nm)	KrF excimer laser(248nm)	Low-press. Hg lamp(254nm)	XeCl excimer laser(308nm)	High-press. Hg lamp(313nm)
$Bi(C_6H_5)_3$*	4.2×10^4	1.6×10^4	1.4×10^4	1.2×10^3	-
$Sr(DPM)_2$	4.0×10^3	5.8×10^3	9.5×10^3	1.3×10^3	0.6×10^3
$Ca(DPM)_2$	3.9×10^3	6.8×10^3	1.0×10^4	1.2×10^3	0.6×10^3
$Cu(DPM)_2$	1.1×10^4	1.7×10^4	1.7×10^4	1.9×10^4	1.6×10^4

(l/mol·cm)

*Value at 1.0×10^{-5}mol/l

Chapter 6

Photo CVD of Metal Oxide Films Relating to Bi-Sr-Ca-Cu-O Superconductor

6-1 Introduction

In chapter 5, the author established the method for the purification of source materials of CVD for high-T_c superconductors. The studies were extended to UV-VIS light absorption property of sources. The author clarified high potential of $Bi(C6H5)_3$, $Sr(DPM)_2$, $Ca(DPM)_2$, and $Cu(DPM)_2$ as photo CVD sources. Most CVD's of high-T_c superconducting film so far reprted have employed thermal decomposition of sources,[1-3] or plasma decomposition using rf[4] or microwave.[5] There are reports neither on the preparation of high-T_c superconducting film nor multilayered film by photo CVD.

In Fig. 6-1, schematic representation of photo CVD process. In the gas phase, A source gas molecule (A in Fig. 6-1) is excited by the photon absorption. The electrochemically excited molecule (A^*) can be decomposed to activated species (X and Y). Secondary reactions of the source gas molecule (A) with these activated species (X and Y) can generate other active species (z) as well. The active species (X, Y, or Z) as a precursor of film deposition is transfered and adsorbed on the surface of film growth. Then the adsorbed precursor (S^*) migrates on the film surface, before it reacts at an active site in solid network (S_n) to be incorporated in the film (S_{n+1}).[6] Improvement of crystallinity of the film could be expected by enhancement of this migration by photon irradiation.[7]

In this chapter, the author reports low temperature

preparation of Bi, Sr, Ca, Cu, and Ca-Cu oxide films by photo CVD using highly purified sources by the method decribed in the chapter 5.

6-2 Experimental

Source materials used were $Bi(C_6H_5)_3$, $Sr(DPM)_2$, $Ca(DPM)_2$, and $Cu(DPM)_2$ complexes which were supplied by Tri-chemical Co., Ltd., Nihonsanso Co., Ltd., and Nihon Kagaku Sangyo Co., Ltd. They were purified by the method described in the author's preceding paper.[8] $Bi(C_6H_5)_3$, $Sr(DPM)_2$, $Ca(DPM)_2$, and $Cu(DPM)_2$ were heated at 120°C, 200°C, 220°C, and 130°C, respectively, and carried through heated stainless pipe into the CVD chamber by Ar(50sccm).

Figure 6-2 depicts schematic diagram of the photo CVD apparatus. Source materials carried with Ar and an oxidant gas (O_2, N_2O, or NO_2; 20sccm) were introduced by separate gas lines. The reaction pressure was 20Torr. The substrate, MgO(100), was placed at 2cm below the quartz window and heated at temperatures between 300°C and 600°C. A low pressure mercury lamp (Orc Co., Ltd.; 110W) was employed as UV light source. The film thickness was measured by the stylus method using ULVAC Dektak-3010. Crystal structure, composition, and surface morphology of the films were measured by X-ray diffraction(XRD, MAC Science: MXP^3) using CuK_α, X-ray photo-electron spectroscopy(XPS, JEOL: JPS-80), and scanning electron microscopy(SEM, JEOL: JSM-T300), respectively. ICP (inductive coupled plasma) emission analysis using SEIKO-SPS1200 model was made to determine the film composition.

6-3 Results and Discussion

6-3-1 Deposition of Bi_2O_3 Film

A thick white film about 1000A was deposited from $Bi(C_6H_5)_3$ at 300°C by photo CVD for 2h, whereas no film was obtained without the UV irradiation. The presence of bismuth, oxygen, and trace of carbon in the film was confirmed by XPS. Figure 6-3 shows XRD pattern of the deposited film. Peaks assignable to (121) and (304) of α-Bi_2O_3 were clearly observed. From the SEM image shown in Fig. 6-4, the film surface was flat and smooth.

6-3-2 Deposition of CuO Film

At substrate temperatures of 300°C and 400°C, black films about 8000A thick were obtained from $Cu(DPM)_2$ in 1h. Figure 6-5 shows XRD patterns of the films prepared (a) at 300°C by photo CVD, (b) at 400°C by thermal CVD, and (c) at 400°C by photo CVD. At a substrate temperature of 300°C, XRD peak was observed in neither of the two films prepared by thermal CVD nor photo CVD. crystalline CuO peaks were observed when the substrate temperature was raised up to 400 C. The peak intensities of CuO prepared by photo CVD were about 1.3~3 times higher than those prepared by thermal CVD, indicating improvement of film crystallinity by the UV irradiation. XPS revealed the divalent state of copper and the presence of oxygen and carbon in the films of Fig. 6-5(b) and (c). The films were not so smooth and pyramidal grains as large as 0.4μm were observed by SEM.(Fig. 6-6)

6-3-3 Deposition of $CaCO_3$ and CaO Film

From $Ca(DPM)_2$ photo CVD gave white films containing calcium, oxygen, and carbon confirmed by XPS. XRD patterns of the films

prepared under various conditions are shown in Fig. 6-7. In the XRD pattern of the film prepared at 300°C, there was no peak(Fig. 6-7(a)). By increasing the substrate temperature to 400°C, (001) oriented $CaCO_3$ films were prepared both by thermal CVD(Fig. 6-7(b)) and photo CVD (Fig. 6-7(c)). The film prepared by photo CVD had the peak intensities higher than the film prepared by thermal CVD. By further increase of substrate temperature to 500°C, strongly (100) oriented CaO films were obtained both with and without UV irradiation (Fig. 6-7(d)), indicating that thermal process was predominant. It is noteworthy that $CaCO_3$ formation was suppressed and CaO formation was promoted at 400°C by using N_2O gas as Fig. 6-7(e) shows. Peak identified to (002) of CaO was observed in the film prepared at 400°C whereas no peak assignable to $CaCO_3$ was observed. SEM images shown in Fig. 6-8 demonstrate that the grains in $CaCO_3$ film prepared at 400°C had diameters less than 0.2μm, far smaller than the grains of about 2μm in the CaO film prepared at 500°C. The reason for the conversion from $CaCO_3$ to CaO by increasing the substrate temperature from 400°C to 500°C will be discussed later.

6-3-4 Deposition of $SrCO_3$ and SrO Film

Figure 6-9 shows XRD patterns of the films prepared from $Sr(DPM)_2$ under various conditions. All these films were confirmed to contain Sr, C, and O by XPS. Peaks assigned to $SrCO_3$ were observed in the XRD patterns of the films prepared at 400°C and 500°C by photo CVD. Without UV irradiation, no XRD peak was observed for the film prepared at 500°C. Films prepared at 500°C and 550°C gave XRD patterns of $SrCO_3$ with (001) orientation more

strongly by using NO_2 gas than by using O_2 gas. At a temperature of 600°C, SrO film was formed irrespective with or without UV irradiation. The temperature required to obtain SrO was higher than CaO, being in good agreement with thermodynamics. From thermodynamic calculation for the following decarbonation reactions;

$$CaCO_3 \rightarrow CaO+CO_2 (\Delta H_f=178.3kJ/mol,\ \Delta S_f=190.3J/mol\cdot K)$$

$$SrCO_3 \rightarrow SrO+CO_2 (\Delta H_f=234.5kJ/mol,\ \Delta S_f=170.6J/mol\cdot K)$$

CaO and SrO should be formed at 517°C and 863°C, respectively. Here, the partial pressure of CO_2 was assumed to be 10^{-4}Torr and that the enthalpy (ΔH) and entropy(ΔS) for the reactions were fixed at the standard values in the temperature range. The substrate temperatures required for the formation of CaO and SrO in this study were slightly lower than the values of this calculation. For better control of product, oxide or carbonate, we should pay more attention to the oxidation condition. Figure 6-10 shows SEM photographs of the films prepared at 500°C(a) and 600°C(b) by photo CVD. Film grown at 500°C has surface, smoother than the film grown at 600°C which is composed of grains about 2μm diameter.

6-3-5 Deposition of Ca-Cu-O Film

The preparation of $CaCuO_2$ attracts the author's interest as a material with Cu-O_2 plane, which is supercurrent layer in high-T_c superconductors,[9] and preliminary study was performed. By simultaneous supply of $Ca(DPM)_2$ and $Cu(DPM)_2$, black films were obtained at a substrate temperature of 400°C both with and without UV irradiations. The deposition rate was about 2.2A/s. Figure 6-11 shows XRD patterns of 8000A films prepared by (a)

photo CVD and (b) thermal CVD. No peak was observed in the film prepared by the thermal CVD, whereas Ca_2CuO_3 was formed by the photo CVD. No peak assignable to $CaCO_3$ or $CaCuO_2$ was detected. Presence of calcium, oxygen, carbon, and divalent state of copper was observed in the photo CVD film by XPS (Fig. 6-12) and the Ca/Cu ratio was determined to be 0.5/1.0 by ICP analysis. Figure 6-13 shows SEM inages of the film of Fig. 6-11(a). On the flat matrix, particles considered to be CuO were observed.

Under the conditions examined, Ca_2CuO_3 was predominantly formed due probably to the higher thermodynamical stability than $CaCuO_2$. It must, however, be noted that the simultaneous supply of $Ca(DPM)_2$ and $Cu(DPM)_2$ resulted in the formation of oxide film, rather than carbonate, since $CaCO_3$ was formed from $Ca(DPM)_2$ under similar conditions.

6-4 Conclusion

Table 6-1 lists prearation conditions and results of this work. UV light irradiation induced crystalline Bi_2O_3 film formation from $Bi(C_6H_5)_3$ at 300°C, whereas no film was obtained without UV light irradiation. $SrCO_3$ was formed at 400°C by photo CVD, whereas amorphous film was obtained under otherwise the same conditions without UV irradiation. Higher crystalline $CaCO_3$ and CuO films were obtained at 400°C by photo CVD than the film prepared by thermal CVD. By simultaneous supply of $Ca(DPM)_2$ and $Cu(DPM)_2$, amorphous and Ca_2CuO_3 films were formed at 400°C by thermal CVD and photo CVD, respectively.

References

1) H. Yamane, H. Masumoto, T. Hirai, H. Iwasaki, K. Watanabe, N.

Kobayashi and Y. Muto: Appl. Phys. Lett., 53 (1988) 1548.

2) S. Oda, H. Zama, T. Ohtsuka, K. Sugiyama and T. Hattori: Jpn. J. Appl. Phys., 28 (1989) L427.

3) K. Natori, S. Yoshizawa, J. Yoshino and H. Kukimoto: Jpn. J. Appl. Phys., 28 (1989) L1578.

4) H. Koinuma, K. Fukuda, M. Kogoma, S. Okazaki, T. Hashimoto, M. Kawasaki and M. Yoshimoto: the Proc. of the 9th Int'l Symp. on Plasma Chem., Pugnochiuso (1989) 1521.

5) T. Hashimoto, K. Kitazawa, T. Kosaka, Y. Yoshida and H. Koinuma: Rep. of the Res. Lab. of Eng. Mater., Tokyo Inst. of Tech., 15 (1990) 97.

6) M. Kawasaki: Dr. Thesis, Univ. of Tokyo (1988) 26.

7) For example, A. Doi, Y. Aoyagi and S. Namba: Appl. Phys. Lett., 48 (1986) 1787.

8) T. Hashimoto, K. Kitazawa, Y. Suemune, T. Yamamoto and H. Koinuma: Jpn. J. Appl. Phys., 29 (1990) L2215.

9) H. Ihara, S. Sugise, T. Shimomura, M. Hirabayashi, N. Terada, M. Jo, K. Hayashi, M. Tokumoto, K. Murata and S. Ohashi: Advances in Superconductivity, Proc. 1st Symp. on Superconductivity (ISS'88), Nagoya, 1988 (Springer-Verlag, Tokyo, 1989) 793.

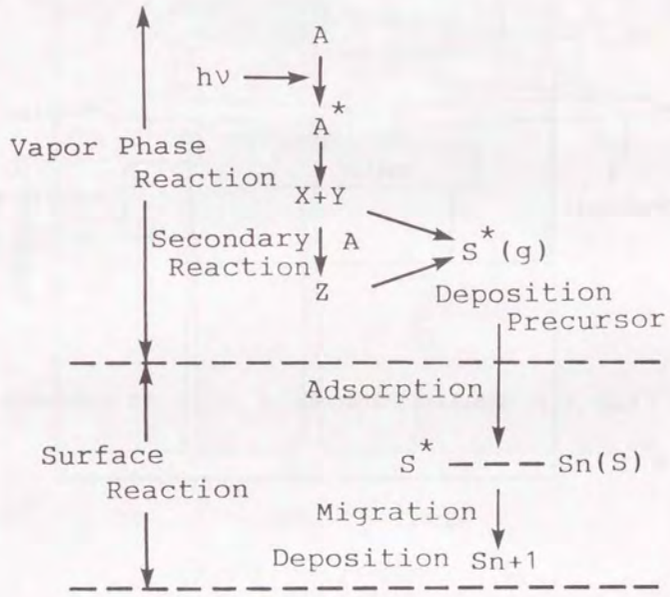

Fig. 6-1. Schematic representation of photo CVD process.

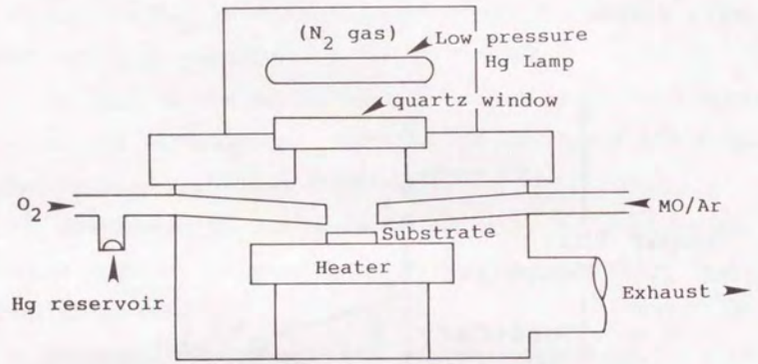

Fig .6-2. Schematic diagram of photo CVD apparatus.

$Bi(C_6H_5)_3$

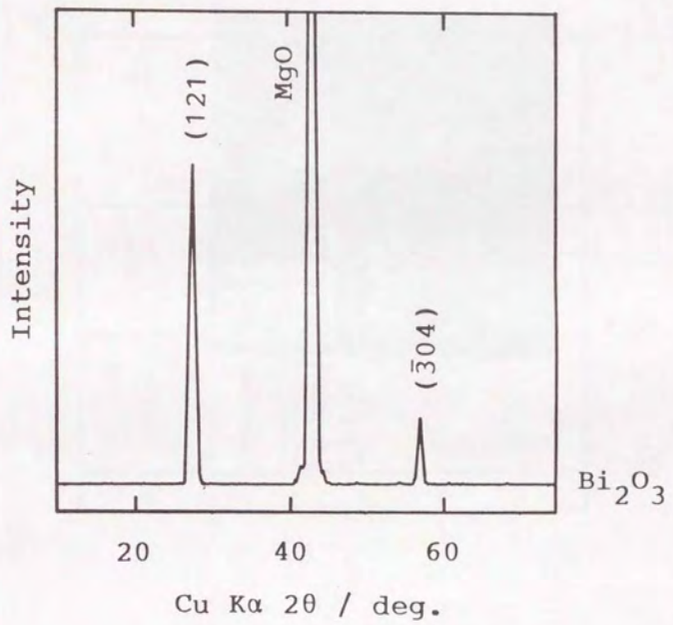

Fig. 6-3. X-ray diffraction pattern of the film prepared from $Bi(C_6H_5)_3$ by photo CVD. The substrate temperature was 300°C.

Fig. 6-4. SEM image of the film prepared from $Bi(C_6H_5)_3$ at 300°C by photo CVD.

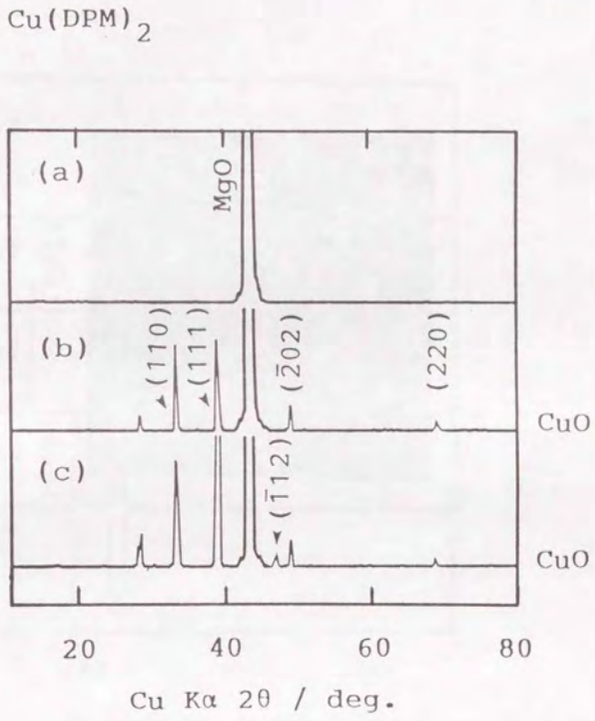

Fig. 6-5. X-ray diffraction patterns of the films prepared from $Cu(DPM)_2$ at (a) substrate temperature of 300°C by photo CVD, (b) 400°C by thermal CVD and (c) 400°C by photo CVD.

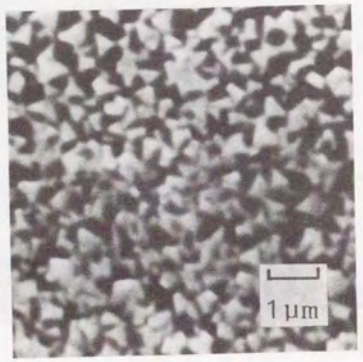

Fig. 6-6. SEM image of the film prepared from $Cu(DPM)_2$ at 400°C by photo CVD.

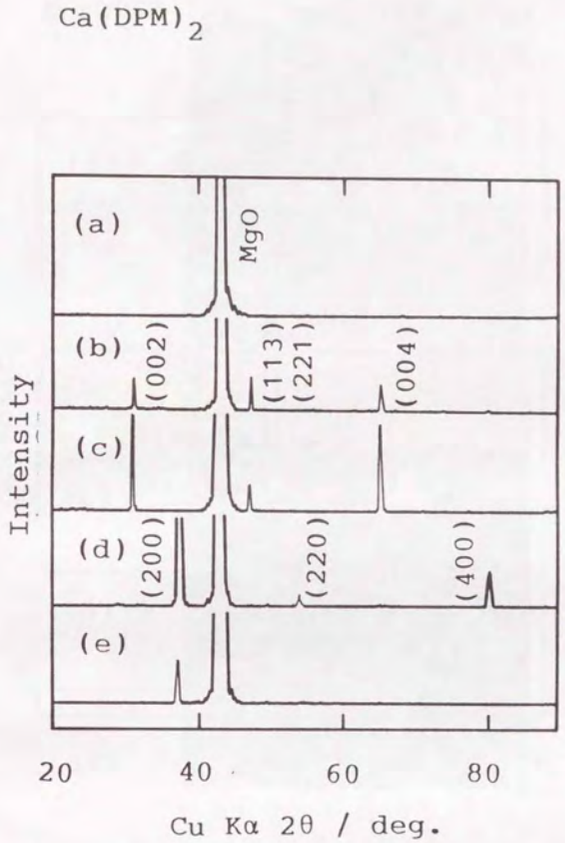

Fig. 6-7. X-ray diffraction patterns of the films prepared from $Ca(DPM)_2$ at (a) 300 °C by photo CVD, (b) 400 °C by thermal CVD, (c) 400 °C by photo CVD, (d) 500° C by photo CVD, and (e) 400 °C by photo CVD using N_2O.

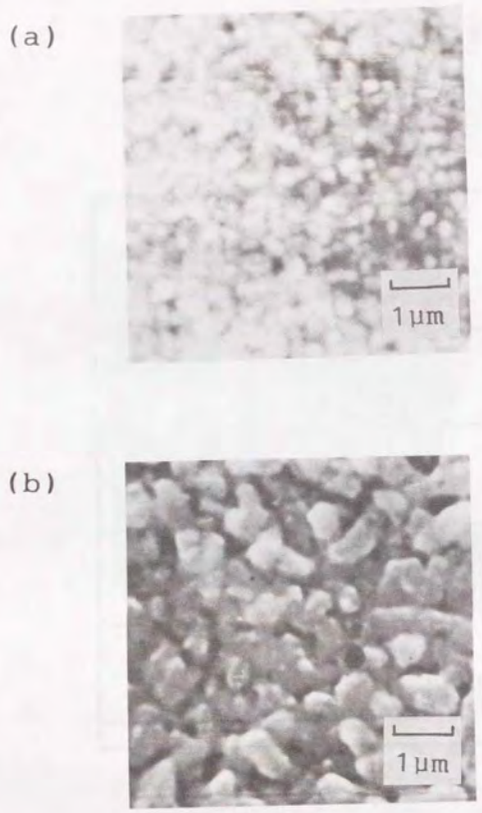

Fig. 6-8. SEM images of the films prepared from $Ca(DPM)_2$ by photo CVD at (a) 400°C and (b) 500°C.

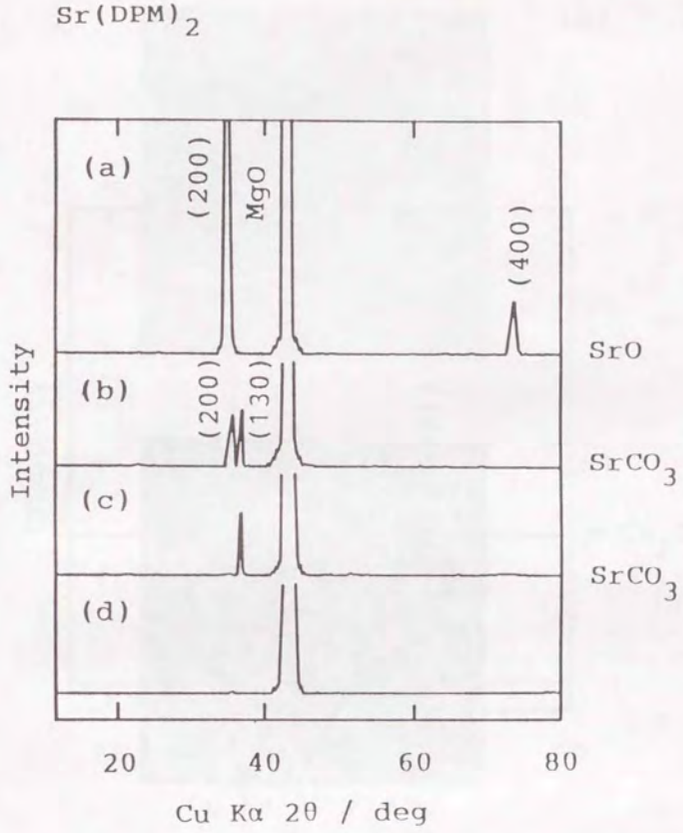

Fig. 6-9. X-ray diffraction patterns of the films prepared from $Sr(DPM)_2$. The preparation conditions are (a) 600°C by photo CVD, (b) 500°C by photo CVD, (c) 400°C by photo CVD, and (d) 500°C by thermal CVD.

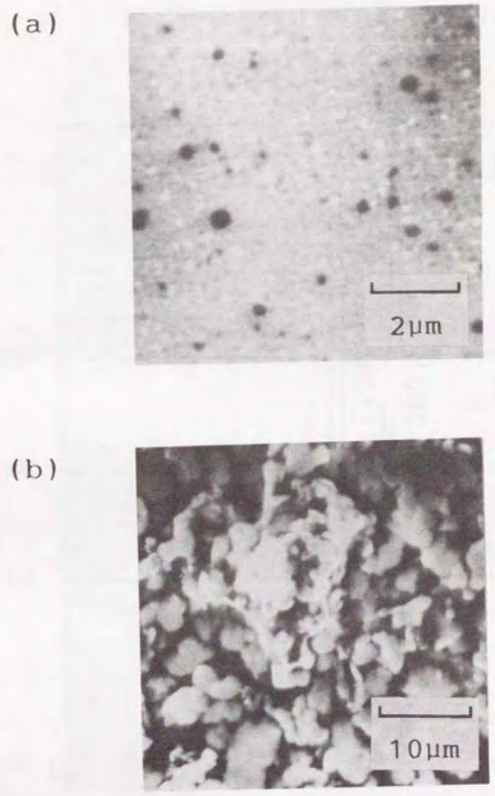

Fig. 6-10. SEM images of the films prepared from $Sr(DPM)_2$ at (a) 500°C and (b) 600°C by photo CVD.

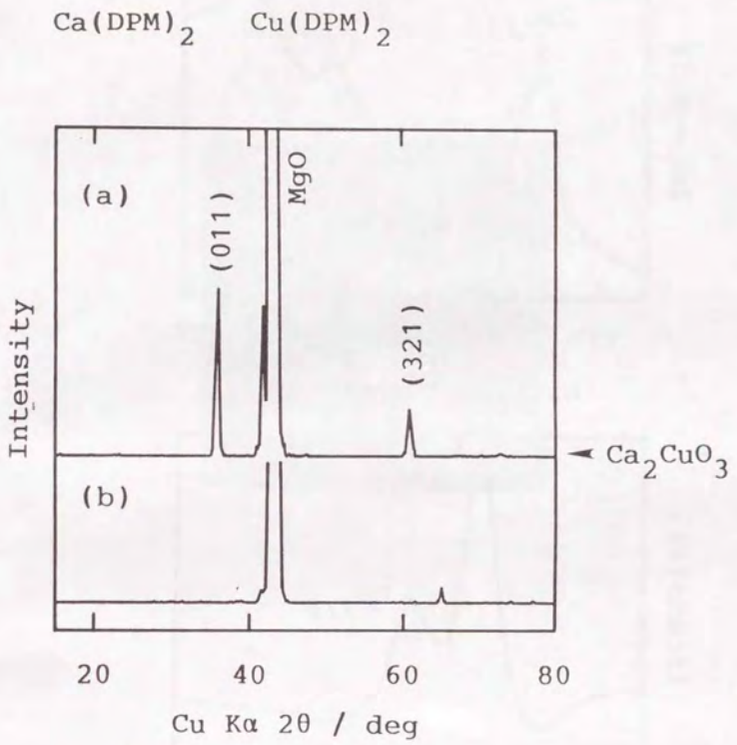

Fig. 6-11. X-ray diffraction patterns of the films prepared at 400 °C by simultaneous supply of $Ca(DPM)_2$ and $Cu(DPM)_2$: (a) photo CVD and (b) thermal CVD.

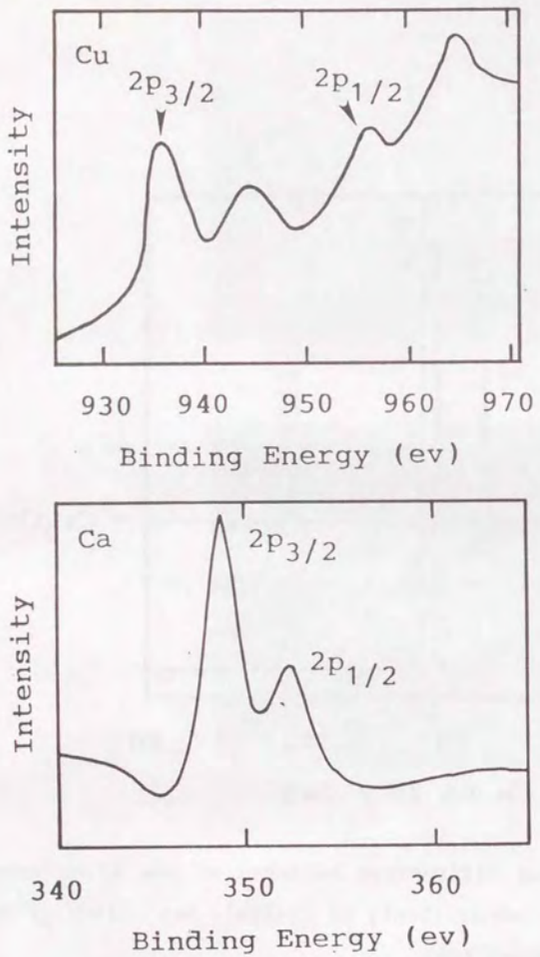

Fig. 6-12. XPS spectra of the film prepared from mixture of $Ca(DPM)_2$ and $Cu(DPM)_2$ at 400 °C by photo CVD.

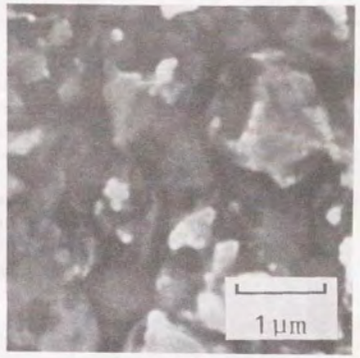

Fig. 6-13. SEM image of the film prepared from mixture of $Ca(DPM)_2$ and $Cu(DPM)_2$ at 400°C by photo CVD.

Table 6-1. Preparation conditions and results of photo CVD

	Source	Oxidation gas flow (sccm)	Sub. temp. (°C)	Crystal structure UV on	Crystal structure UV off	Comment
#1	$Bi(C_6H_5)_3$	O_2: 20	300	Bi_2O_3	no film	
#2	$Cu(DPM)_2$	O_2: 20	300	amorphous	amorphous	
#3	$Cu(DPM)_2$	O_2: 20	400	CuO	CuO	higher XRD peak intensity by UV irradiation
#4	$Cu(DPM)_2$	N_2O: 20	400	CuO	-	(110) orientation
#5	$Ca(DPM)_2$	O_2: 20	400	$CaCO_3$	$CaCO_3$	higher XRD peak intensity by UV irradiation
#6	$Ca(DPM)_2$	O_2: 20	500	CaO	CaO	high (100) orientation
#7	$Ca(DPM)_2$	N_2O: 20	400	CaO	amorphous	CaO(200) peak was observed
#8	$Sr(DPM)_2$	O_2: 20	500	$SrCO_3$	amorphous	
#9	$Sr(DPM)_2$	O_2: 20	600	SrO	SrO	high (100) orientation
#10	$Sr(DPM)_2$ $Ca(DPM)_2$	NO_2: 20	500	$SrCO_3$	-	high (001) orientation
#11	& $Cu(DPM)_2$	O_2: 20	400	Ca_2CuO_3	amorphous	carbonate was not observed

Reaction Pressure: 20Torr Ar flow: 50sccm

Chapter 7

General Conclusion

(1) High-T_c superconducting thick films were successfully prepared by screen printing/sintering method. Maximum T_c, zero were observed 25K, 83K, and 68K for LSCO, BYbCO, and BSCCO, respectively. Properties of the films were highly dependent on substrate materials.

(2) Physical and chemical interactions between high-T_c superconducting oxide and substrate materials were clarified semi-quantitatively. Thermal expansion coefficients of superconductors were verified to be higher than conventionally used substrate materials. Alkaline earth elements in high-T_c superconductors easily reacted substrate materials in solid state at high temperatures. MgO and $SrTiO_3$ were confirmed to be suitable as substrates for superconducting film.

(3) The purification methods of sources for CVD of high-T_c superconducting film were established. Thermal and light absorption properties of the sources were also clarified. Application of plasma or UV irradiation to CVD of oxide film was confirmed to be effective to decrease substrate temperature.

Publication List

Original Papers

Screen Printing

(1) "Preparation of $(La_{1-x}Sr_x)_2CuO_{4-\delta}$ Superconducting Films by Screen Printing Method" H. Koinuma, T. Hashimoto, M. Kawasaki, and K. Fueki: Jpn. J. Appl. Phys., 26 (1987) L399.
(2) "High-T_c Superconductivity in Screen Printed Yb-Ba-Cu-O Films" H. Koinuma, T. Hashimoto, T. Nakamura, K. Kishio, K. Kitazawa and K. Fueki: Jpn. J. Appl. Phys., 26 (1987) L761.
(3) "Superconductivity and Substrate Interaction of Screen Printed Bi-Sr-Ca-Cu-O Films" T. Hashimoto, T. Kosaka, Y. Yoshida, K. Fueki and H. Koinuma: Jpn. J. Appl. Phys., 27 (1988) L384.
(4) "Screen-Printing/Sintering as a Preparation Method of Oxide Superconducting Films" H. Koinuma and T. Hashimoto: Anual Rep. of the Eng. Res. Inst. Fac. of Eng., Univ. of Tokyo 47 (1988) 139.
(5) "Preparation of a Bi-Sr-Ca-Cu-O High-T_c Superconductor by the Reaction of A Cu Free Precursor with Cu Plate" M. Yoshimoto, T. Hashimoto and H. Koinuma: Jpn. J. Appl. Phys., 28 (1989) L984.

Interaction between Superconductor and Substrate Materials

(6) "Some Problems in the Preparation of Superconducting Oxide Films on Ceramic Substrates" H. Koinuma, M. Kawasaki, T. Hashimoto, S. Nagata, K. Kitazawa, K. Fueki, K. Masubuchi and M. Kudo: Jpn. J. Appl. Phys., 26 (1987) L763.
(7) "Thermal Expansion Coefficients of High-T_c Superconductors" T. Hashimoto, K. Fueki, A. Kishi, T. Azumi and H. Koinuma: Jpn. J. Appl. Phys., 27 (1988) L214.
(8) "Interaction of La-Sr-Cu-O and Ln-Ba-Cu-O (Ln=Y, Ho, Yb) Films with Ceramic Substrate" H. Koinuma, T. Hashimoto, M. Kawasaki, K. Kitazawa, K. Fueki, A. Inoue and Y. Okabe: SPIE vol. 948 High-T_c Superconductivity: Thin Films and Devices (1988) 25.
(9) "Chemical Interaction between $Ba_2YCu_3O_{7-\delta}$ and Substrate Materials in the Solid State" H. Koinuma, K. Fukuda, T. Hashimoto and K. Fueki: Jpn. J. Appl. Phys., 27 (1988) L1216.
(10) "Solid Phase Reaction of Oxide Superconductors with Ceramic Substrate Materials" T. Hashimoto, T. Yoshida, M. Yoshimoto, M. Takata and H. Koinuma: Rep. of the Res. Lab. of Eng. Mater. Tokyo Inst. of Tech., 14 (1989) 91.
(11) "Chemical Interaction between High-T_c Superconducting Oxides and Alkaline Earth Fluorides" T. Hashimoto, T. Asakawa, T. Shiraishi, T. Yoshida, M. Yoshimoto and H. Koinuma: Jpn. J. Appl. Phys., 28 (1989) L1156.

CVD

(12) "Plasma Chemical Vapor Deposition of Metal Oxide Thin Films Relating to High-T_c Superconductor" M. Yoshimoto, T. Hashimoto, K. Kosaka, K. Fukuda, M. Kogoma, S. Okazaki, T. Asakawa, M. Kawasaki and H. Koinuma: Proc. of the 6th Plasma Processing, Kyoto, (1989) 365.
(13) "Preparation of Bi, Sr, Ca and Cu Oxide Films by rf Plasma MOCVD" H. Koinuma, K. Fukuda, M. Kogoma, S. Okazaki, T. Hashimoto, M. Kawasaki and H. Koinuma: Proc. of the 9th Int'l Symp. on Plasma Chem., Pugnochiuso, Italy, 3 (1989) 1521.
(14) "Deposition of Bi, Sr, Ca and Cu Oxide Films by rf Glow Discharge Generated at Relatively High Pressure" T. Hashimoto, K. Fukuda, M. Kogoma, S. Okazaki, M. Yoshimoto and H. Koinuma: Mol. Cryst. Liq. Cryst., 184 (1990) 201.
(15) "Microwave Plasma CVD of Oxide Films Relating to High-T_c Bi-Sr-Ca-Cu-O Superconductors" T. Hashimoto, T. Kosaka, Y. Yoshida and H. Koinuma: Mol. Cryst. Liq. Cryst., 184 (1990) 207.
(16) "Plasma Assisted Chemical Vapor Deposition of Thin Films Related to High-T_c Oxide Superconductor" T. Hashimoto, K. Kitazawa, T. Kosaka, Y. Yoshida and H. Koinuma: Rep. of the Res. Lab. of Eng. Mater., Tokyo Inst. of Tech., 15 (1990) 97.
(17) "Purification and UV-VIS Light Absorption Property of Source Materials for CVD of High-T_c Superconducting Films" T. Hashimoto, K. Kitazawa, Y. Suemune. T. Yamamoto and H. Koinuma: Jpn. J. Appl. Phys., 29 (1990) L2215.
(18) "Photo CVD of Metal Oxide Films Relating to Bi-Sr-Ca-Cu-O Superconductor" H. Koinuma, K. A. Chaudhary, M. Nakabayashi, T. Shiraishi, T. Hashimoto, K. Kitazawa Y. Suemune and T. Yamamoto: to be published in Jpn. J. Appl. Phys.

Laser Processing of High-T_c Superconducting Films

(19) "Reversible Resistivity Control of $Ba_2YCu_3O_{7-}$ Thin Films by Laser Annealing" H. Koinuma, Y. Takemura, T. Hashimoto, K. Takeuchi and K. Fueki: Jpn J. Appl. Phys., 27 (1988) L652.
(20) "Laser Processing of $Ba_2YCu_3O_{7-}$ Films" H. Koinuma, Y. Takemura and T. Hashimoto: Anual Rep. of the Eng. Res. Inst. Fac. of Eng., Univ. of Tokyo, 47 (1988) 145.

New Superconductor

(21) "Superconductivity in a New Oxide System of Eu-La-Ce-Cu-O" M. Yoshimoto, T. Hashimoto, M. Takata and H. Koinuma: Jpn. J. Appl. Phys., 28 (1989) L1115.
(22) "Superconductivity in Eu-La-Ce-Cu-O System" H. Koinuma, M. Yoshimoto, T. Hashimoto and M. Takata: Mol. Cryst. Liq. Cryst., 184 (1990) 183.

Coating of Superconducting Film

(23) "Stabilization of $Ba_2YCu_3O_{7-}$ by Surface Coating with Plasma Polymerized Fluorocarbon Film" K. Sato, S. Omae, K. Kojima, T. Hashimoto and H. Koinuma: Jpn. J. Appl. Phys., 27 (1988) L2088.

Diamond and Carbon Films

(24) "Effect of Nitrous Oxide Gas on CVD Diamond Film Deposition" H. Koinuma, M. Yoshimoto, Y. Takagi, A. B. Sawaoka, T. Hashimoto, T. Nagai and T. Shiraishi: to be published in the Proc. of 1990 MRS Spring Meeting.
(25) "Cemical Vapor Deposition of Carbon Films Assisted with rf glow Discharge at Moderately High Pressures" K. Inomata, T. Shiraishi, T. Hashimoto, M. Kogoma, S. Okazaki and H. Koinuma: to be published in Rep. of the Res. Lab. of Eng. Mater., Tokyo Inst. of Tech., 16 (1991).

Amorphous Semiconductor

(26) "Fluorosilanes for Plasma- and Photo-CVD's: A search by Molecular Orbital Methods" T. Hirano, T. Manako, T. Hashimoto, K. Fueki and H. Koinuma: Proc. of the 8th Int'l Symp. on Plasma

Chem., Tokyo, (1987) 1502.

Laser MBE
(27) "Fabrication by Laser MBE and in situ Characterization of Layered Cuprates" H. Koinuma, H. Nagata, T. Hashimoto, T. Tsukahara, S. Gonda and M. Yoshimoto: to be published in the 3rd Int'l Symp. on Superconductivity, Sendai, (1990).
(28) " In situ RHEED and XPS Studies on Ceramic Layer Epitaxy in UHV System" H. Koinuma, M. Yoshimoto, H. Nagata, T. Hashimoto, T. Tsukahara, S. Gonda, S. Watanabe, M. Kawai and T. Hanada: to be published in the Proc. of the 4th Annual Conf. on Superconductivity and Applications, Buffalo, New York (1990)
(29) " Preparation of Oxide Films in Ultra High Vacuum System" T. Tsukahara, M. Yoshimoto, H. Nagata, T. Hashimoto, S. Gonda and H. Koinuma: submitted to Int'l Symp. on Solid State Chemistry of Advanced Materials, Workshop on Non-stoichiometric Compounds, Tokyo (1990); to be published in Solid State Ionics.

Books and Reviews(in Japanese)

(1) "Preparation of Ceramic Superconducting Films" T. Hashimoto, K. Fueki and H. Koinuma: Highlight of Advanced Technology No. 54 (1987) 1.
(2) "Preparation of High-T_c Oxide Superconductors-Fabrication of Thick Films" T. Hashimoto and H. Koinuma: Oyo Buturi (Applied Physics) 57 (1988) 1225.
(3) "Preparation of Superconducting Films by Screen Printing Method" K. Fueki, H. Koinuma and T. Hashimoto: Screen Printing 250 (1988) 70.
(4) "Thermal Expansion Coefficients of High-T_c Superconductors" T. Hashimoto, H. Koinuma and A. Kishi in "Chemistry of Oxide Superconductor", eds., K. Fueki and K. Kitazawa, Kodansha Scientific, Tokyo, (1988) p217.
(5) "Cross Section and Spectra of CVD Sources" H. Koinuma and T. Hashimoto in "Handbook of Photo Excitaion Process", eds., K. Takahashi and M. Konagai, Science Forum, Tokyo, (1987) 19.
(6) "Preparation of Superconducting Thin Films by CVD" T. Hashimoto, T. Kosaka and H. Koinuma: Material Analysis and Characterization Science, 4 (1990) 13.
(7) "Surface Processes in Photo-Excited Thin Film Technology" H. Koinuma and T. Hashimoto in "Chemistry of Surface Excitation Process" ed. Chemical Society of Japan, in press.

Films Relating to High-Tc Superconductors 「超伝導関連酸化物薄膜作製の物理化学的研究」